Synthesis of Polypyrrole Coated Copper Nanowire and Its Application as Hydrogen Peroxide Sensor

by

Yang Liu

A thesis submitted to the Graduate Faculty of
Auburn University
in partial fulfillment of the
requirements for the Degree of
Master of Science

Auburn, Alabama
December 12, 2011

Keywords: Copper, Nanowire, Polypyrrole Coating, H_2O_2 Sensing

Approved by

Xinyu Zhang, Chair, Assistant Professor of Polymer and Fiber Engineering
Peter Schwartz, Professor of Polymer and Fiber Engineering
Sabit Adanur, Professor of Polymer and Fiber Engineering
Maria Lujan Auad, Associate Professor of Polymer and Fiber Engineering

Abstract

Polypyrrole coated copper nanowire was synthesized by a metal-organic complex route in one-pot manner. The as-synthesized copper nanowires were single crystalline which grew along the {110} direction with {111} facets exposed on the surface. A layer of polypyrrole coating with a thickness of 5-6 nm could also be observed on the surface of the nanowires, as confirmed by HRTEM. Based on the real-time monitoring of the spectral and electrochemical potential change for the synthetic process, it was believed that a synergistic crystal growth and polymerization effect eventually led to the formation of the polypyrrole coated copper nanowire. The ligand-to-metal charge transfer (LMCT) excitation between pyrrole and the cupric central ion, along with the capping effect of polypyrrole would attribute significantly during this formation process. However, the electrochemical properties of the copper nanowires did not alter notably with the presence of polypyrrole coating, and they also exhibit sufficient electrocatalytic property towards hydrogen peroxide reduction in phosphate buffer solution. A potentiometric sensor based on the copper nanowire modified graphite electrode was therefore fabricated to investigate the sensory ability of the copper nanowires to hydrogen peroxide. The modified electrode exhibited high selectivity and sensitivity of 180.65 mV/mM to hydrogen peroxide, unambiguously revealing the excellent sensory properties of the as-synthesized copper nanowire to hydrogen peroxide. The copper nanowire also exhibited substantially enhanced anti-corrosion properties compared to the uncoated sample, which unraveled the unprecedented application

potential for the copper nanowires in sensors, catalysts, and nanoelectronics, as a result of its excellent electrochemical activity and environmental stability.

Acknowledgments

The author gratefully thanks to the bounteous support and advices from Dr. Xinyu Zhang. Also expressively thanks to Zhen Liu with his countless help for a successful completion of this thesis work. The author also wants to thank his family, who give him boundless encouragement and bravery for completing this faithful task. It is also necessary to acknowledge the whole faculty and staff in the Polymer & Fiber Engineering department, as well as the graduate students, for their genuine help and support corresponding to the author's work.

Table of Contents

List of Tables

List of Figures

Chapter 1

Copper Nanocrystals and Their Application as Sensory Materials

1.1. Introduction

Metal Nanocrystals (MNCs) have attracted extensive research attention within decades for their unique electronic, catalytic, and sensory properties. They may serve as interconnections for nanodevices,[1] substrate for high performance catalysts,[2] and active species for sensory materials.[3] The unique properties of the MNCs could be ascribed to their excellent electron transfer abilities inherent from the bulk counterpart as well as the ultra-high surface area derived from their nanoscale size.[4] Among various kinds of MNCs, the ones of noble metals, such as Pt, Pd, Au, Ag, are under substantial scientific investigation as a result of their outstanding environmental stability and catalytic properties toward a diversity of reactions.[5] Nanocrystals including nanoparticles, rods, wires, cubes, octahedrons of these noble metals have been numerously synthesized and their catalytic properties upon various species and analytes have also been revealed.[6]

Besides noble metals, base metals such as Cu, Ni, Co, Mo and Re also possess distinguished catalytic activities for a good many of specific reactions and analytes.[7] Compared to noble metals, these base metals have indeed attained the advantages of bearing high efficiency for

specific chemical reactions, ease of chemical modification and relative low price.[8] Similar to the case of noble metals, nanocrystals with varying morphologies (rods, tubes, dendrites, etc.) regarding these base metals have also been extensively synthesized, and their applications as heterogeneous catalytic systems are of a common interest among the scientists.

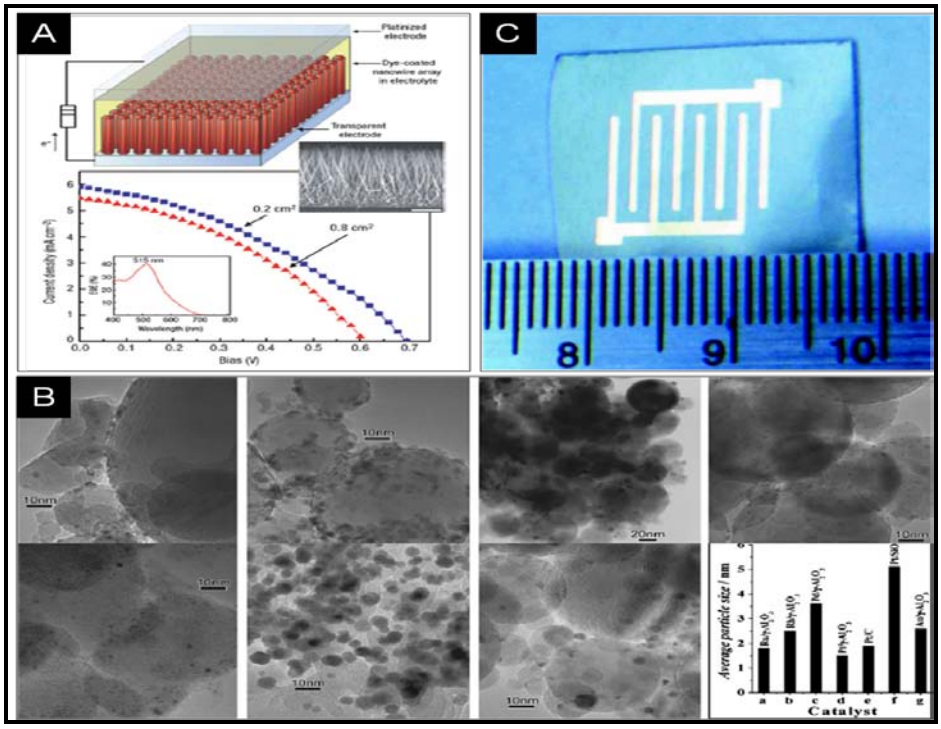

Figure 1. (A) Schematic diagram of ZnO nanoarray dye-sensitized solar cell (DSSC).[1] (B) TEM micrographs for Ru/γ-Al_2O_3, Rh/ γ-Al_2O_3, Pd/ γ-Al_2O_3, Pt/ γ-Al_2O_3 (from left to right, upper column); and Pt/C, Pt/SiO_2, Au/ γ-Al_2O_3 catalysts (2 wt.%) along with their average particle size distribution (from left to right, lower column).[2] (C) Digital image of an impedance-based interdigital nanoporous alumina humidity sensor.[3]

1.2. Types of Copper Nanocrystals

Copper nanocrystals (Cu NCs) could be separated into different categories based on their nature of crystallization and morphologies. However, they could either be single or polycrystalline, depending on the consistency of the fringe space on the crystal. Single crystalline Cu NCs are uniformly composed of crystal lattices with fringe space of approximate 2.1 Å;[13] on the other hand, polycrystalline Cu NCs are composed of lattices with different fringe

space, which are deviated from the standard value of 2.1 Å. In general, single crystalline Cu NCs are more favorable in practical trials due to it would have less grain boundaries and defects which raise the energy barrier for electron transfer.[14]

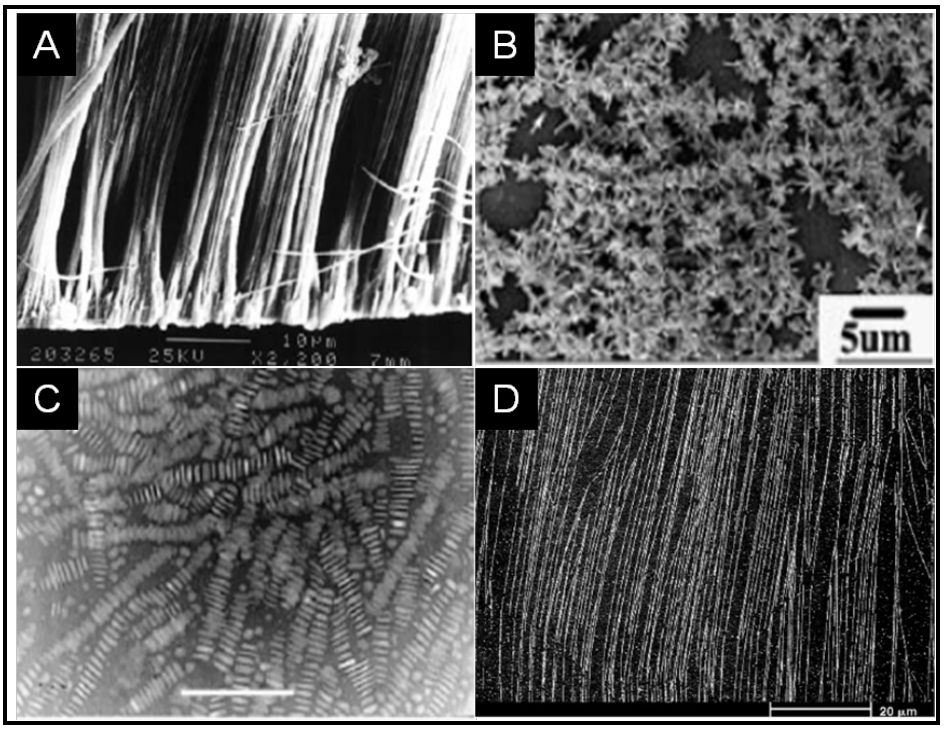

Figure 2. (A) SEM image of cross-section view of copper nanowires synthesized by electrochemical deposition (ECD).[9] (B) SEM image of nickel nanoflowers synthesized by chemical reduction.[10] (C) TEM image of cobalt nanorods synthesized in a binary surfactant system.[11] Scale bar: 100 nm. (D) SEM image of molybdenum nanowires synthesized by electrodeposition. [12]

Other than their crystalline nature, Cu NCs could also be classified according to their distinct morphologies. Typical morphologies for Cu NCs include particles, rods, wires, dendrites, and flowers. Based on the shape and aspect ratio of these morphologies, one could easily differentiate one kind of Cu NCs from the other, or named the existing Cu NCs with an appropriate name. Properties of CuNCs are majorly determined by their morphologies and crystalline nature as well. NCs with distinct morphologies would possess specific surface

characteristics and energy distribution, thus giving themselves diverse properties in surface plasmon, sensing activity, and heterogeneous catalytic system.[15] On the other hand, crystalline homogeneity would affect the NCs' properties such as electron transfer efficiency, thermal conductivity, and dimensional stability;[16] the different exposure facets of the NCs have also been considered as the one of the most essential factors in controlling the efficiency and selectivity of the NC based catalysts and sensory materials.[17]

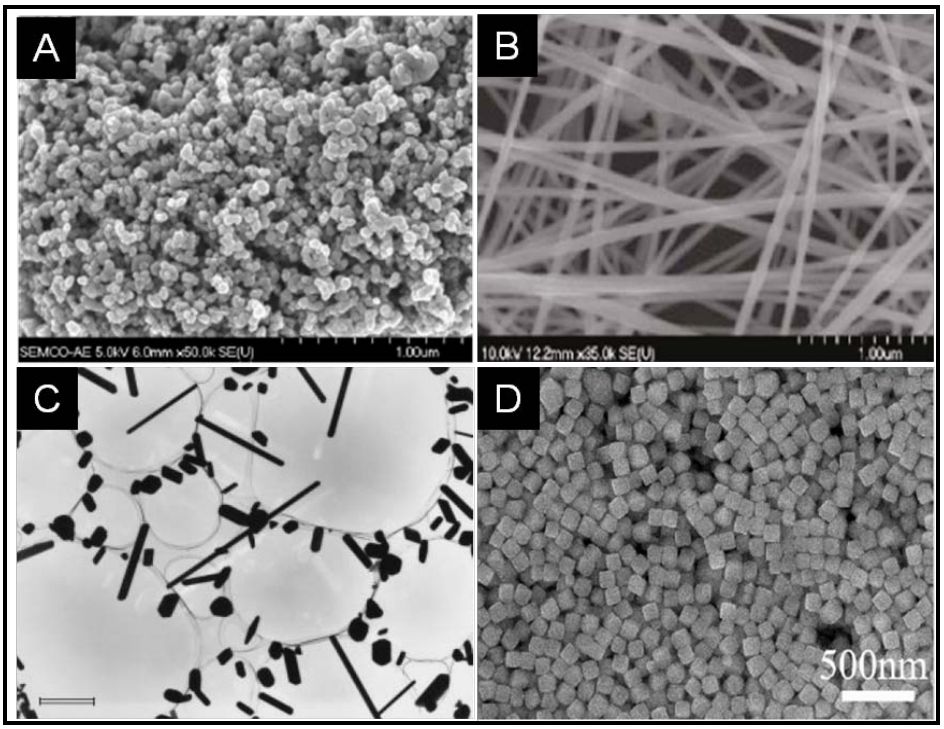

Figure 3. (A) FE-SEM image of copper nanoparticles synthesized by chemical reduction.[18] (B) SEM image of copper nanowires synthesized by hydrothermal reduction with glucose.[19] (C) TEM image of copper nanorods prepared by vacuum vapor deposition method (VVD).[20] Scale bar: 100 nm. (D) SEM image of copper nanocubes prepared by hydrothermal reduction with ascorbic acid.[21]

1.3. Copper Nanowires and Its Sensory Applications

It has long been speculated that metallic nanowire arrays could found significant application potential as sensory materials in fabricating optical,[22] gas,[23] pH,[24] and biomedical sensors.[25] However, the metallic nanowire arrays possess superior sensory properties deriving from their high density interconnected network, open network accessibility, and dimensional regularity.[26]

The high density interconnected network of the nanoarrays would undoubtedly amplify the interaction between the metallic substrate and the stimuli; on the other hand, large open network accessibility would enhance the diffusion process of the stimuli through the network and thus giving a higher possibility for the effective interaction between the substrate and stimuli to occur.[27] The combination of these two effects generally raises a much higher sensitivity that could be expected from the metallic nanowire arrays, corresponding to certain groups of stimuli and types of sensor. Nevertheless, the high dimensional regularity of the nanowire arrays, which could be referred to as the low polydispersity of the crystal facet distribution, would otherwise endow the nanowire arrays with unprecedented selectivity.[28] In other words, the crystal facets of metallic nanowire arrays are majorly composed of the cross-sectional facet (mostly {111}) and the lateral dimensional facet (mostly {100}), and the ratio between the lateral one and the cross-sectional one is always high, indicating the monotonic distribution of the facet composition.[13, 19,29] Thus the nanowire arrays could be highly selective to certain stimuli which would be more favorably to adsorb or coordinate onto either the cross-sectional facet or the lateral dimensional facet.[28] Furthermore, the selectivity of the nanowire arrays could be fine-tuned by controlling the aspect ratio of the nanowire arrays, which enables the nanowire arrays with significant practical flexibility.

As one of the most frequently used metallic materials in engineering the infrastructures, copper has its distinguished properties compared to other metals based on its high electrical/thermal conductivity, reactivity, and nature abundance.[29] Therefore, copper nanowire arrays would be expected to have outstanding sensory properties ascribing to the excellent electrochemical activity of the copper substrate and the open interconnected network morphology. It has been evident that copper nanowires could be utilized as highly sensitive giant

magnetoresistance (GMR) sensor for testing the GMR of the electronics;[30] they are also able to form core-shell structures via in-situ generation of CuO sheath on the surface, which exhibit notable hydrogen, photon, and pH sensing response at room temperature;[31] bi-metallic alloy nanowires of copper and germinate has also been synthesized, which shows excellent sensing properties to cysteine at room temperature;[32] after all, copper nanowires could also be utilized as molecular sensor, which could sense the target molecules adsorb onto their surface through conductance quantization.[33]

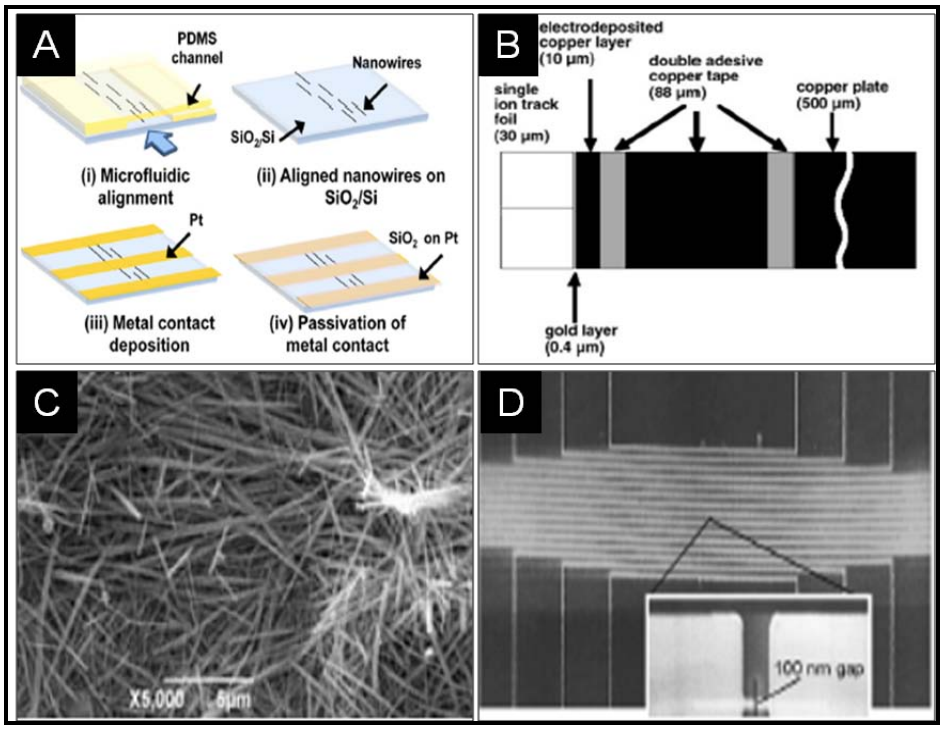

Figure 4. (A) Fabrication processes of Cu-CuO core-shell nanowire sensor.[31] (B) Fabrication processes of Cu nanowire GMR sensor.[30] (C) SEM image of the as-prepared Cu-Ge bimetallic nanowires.[32] (D) SEM image of the molecular sensor based on conductance quantization of Cu nanowires.[33]

Chapter 2

Characteristics of Polypyrrole and Its Application as Coating Material

2.1. Characteristics of Polypyrrole

As one of the most important members in conducting polymer family, polypyrrole has its own unique characteristics differing from the other conducting polymers, recognized by its high conductivity, electrochemical activity, stability, and biocompactibility.[34] Due to its excellent properties, polypyrrole has been under extensively investigation for its application in electronic and electroactive materials, such as field effect transistors, electroluminescent diodes, and electromagnetic shielding layers.[35] On the other hand, polypyrrole has also been fabricated into varying types of advanced form, such as self assemble monolayers (SAM), Langmuir-Blodgett films, and nanoarchitectures, in order to investigate the morphology-dependent properties of polypyrrole and possibly precise control of the polymer properties through alternating morphologies.[36] However, polypyrrole has also been subject to be one of the components of various composite and electrode materials, functioning from the conductive substrate, biological binders, to protective layers.[37]

In general, polypyrrole could be referred to as the polymers formed through the polymerization of pyrrole or its derivatives. The most common polypyrrole was produced solely form pristine pyrrole and pyrrole derivatives are barely used in practical production of pyrrole,

only if certain special application requirements have been specific (solubility, meltability, dispersibility, etc.). Polypyrrole could be produced through varying kinds of methods including electrochemical, oxidation, plasma, and irradiation polymerization, among of which the electrochemical and oxidation methods are most frequent utilized.[34] The polymerization of pyrrole majorly follows the free radical cationic mechanism, which is generally composed of three synthetic steps namely initiation, propagation, and termination.[38] When an electron is taken from the pyrrole monomer by the oxidants or current flow, a pyrrole radical cation would form, and it would initiate the polymerization through the coupling with another pyrrole monomer.

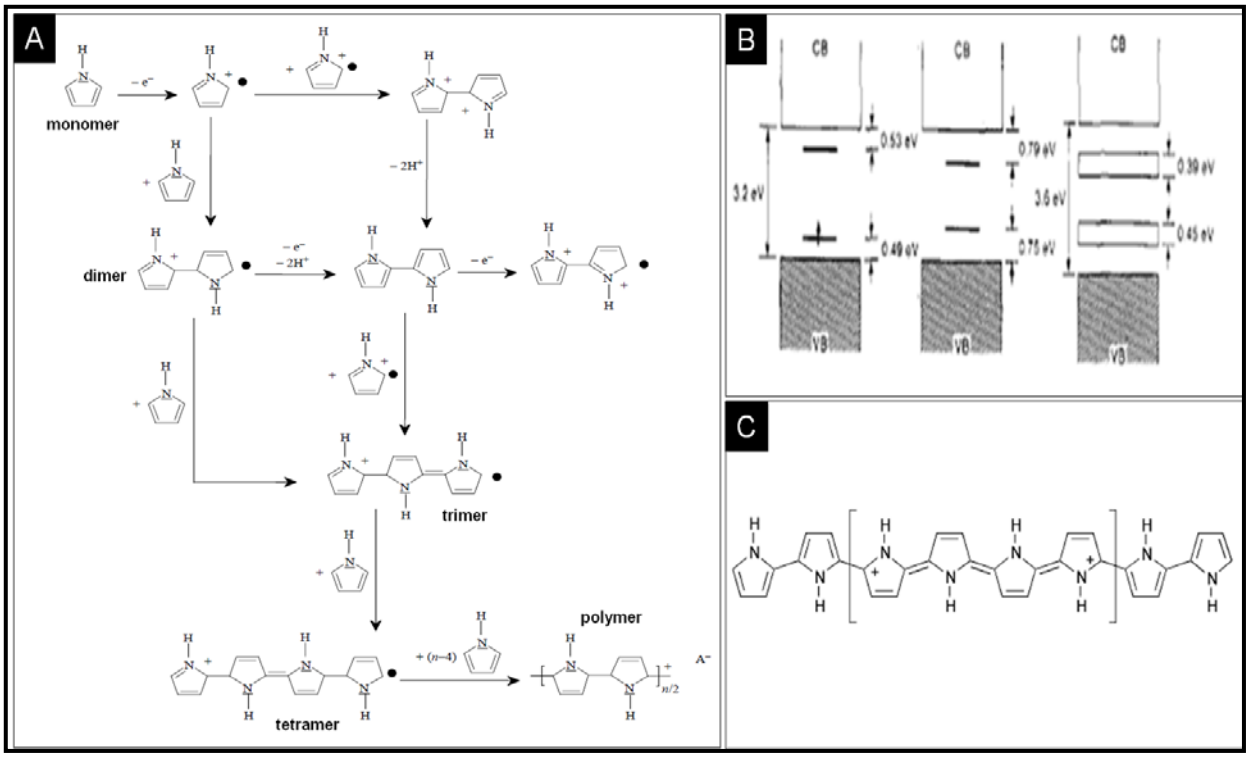

Figure 5. (A) Polymerization mechanism of polypyrrole.[34] (B) Evolution of polypyrrole band structure upon doping. From left to right: low doping level, polaron formation; moderate doping level, bipolaron formation; high doping level (33 mol%), formation of bipolaron bands.[39] (C) Molecular structure of polypyrrole.[41]

This coupling process would continue generating radical dimmers, trimmers, tetramers with active chain ends which would eventually lead to the formation of the long-chain polypyrrole. The thus-formed polypyrrole is majorly composed of polymer backbones with alternating single

and double bonds, which are normally referred to as the π conjugated system.[34] Excess amount of oxidative dopants are normally required to create oxidation defects along the polymer backbone, which would result in the formation of polarons and bipolarons localized within certain distorted chain portions composed of four pyrrole rings.[39] Quinoid-like pyrrole rings also exist within the distorted portions in order to link the charge components of the polarons/bipolarons together. The existing of polarons/bipolarons within the polymer backbones would create a new electronic state for the polymer, located between the valence band and conduction band, which enables charge transfer through these states and facilitates the conducting properties of the polymer backbone.[39] Furthermore, the conductivity of polypyrrole could be controlled by varying the oxidation state of the polymer backbones, on the basis of not deteriorating their conjugated conformation.[40] Higher oxidation state would create more polarons/bipolarons as well as increasing the energy range of the electronic states, which would eventually lead to the new band formation and enhance the conductivity substantially.[39]

2.2. Application of Polypyrrole as Coating Materials

Polypyrrole has been widely investigated as coating materials on various substrates as a result of its extraordinary conducting and electrochemical properties.[44] Polypyrrole coating is believed to be capable of endowing the substrate with distinct electrical/electronic properties through interfacial charge transfer interaction.[42] Generally speaking, polypyrrole coating could be utilized to alter the conductivity of the substrate, which is able to make the intrinsic insulating substrates (polystyrene, PET, etc.) become conductive;[43] on the other hand, it's also widely

adapted to achieve electronic state modification of the substrate. Several materials such as carbon nanotubes, silicon nanowires, and PbSe nanocrystals, their electronic states could be engineered substantially with polypyrrole coating, which facilitates an effective route to control the charge transfer and field emission properties of these materials.[43,44]

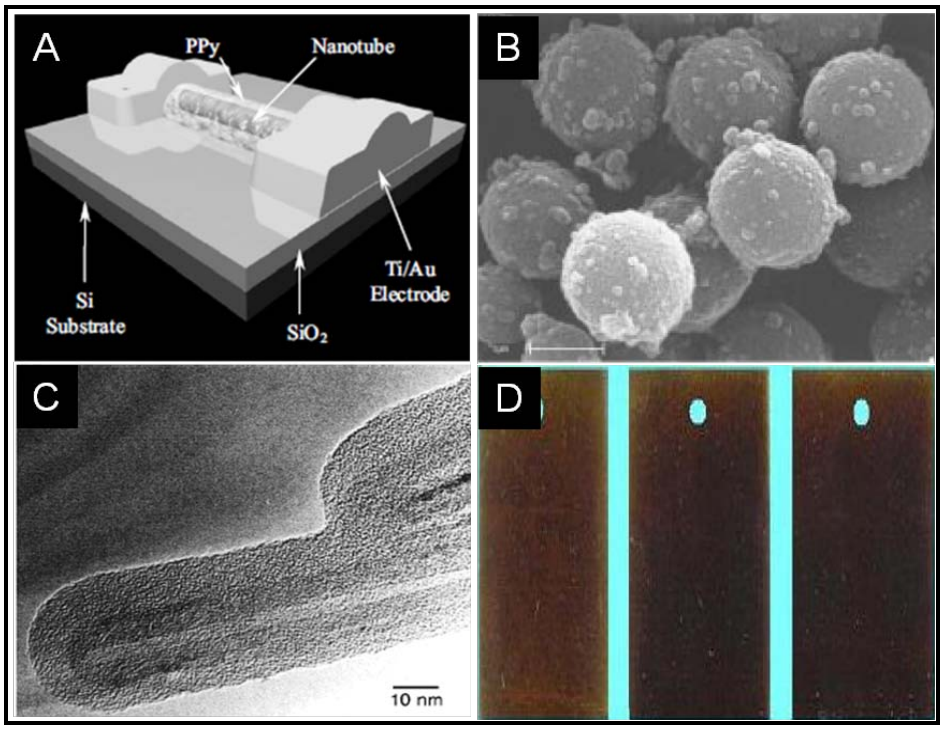

Figure 6. (A) Illustration of an individual SWCNT/PPy composite nanocable device.[42] (B) SEM image of polypyrrole coated polystyrene latex with polypyrrole loading of 25.1%.[43] (C) HRTEM image of two parallel nanotubes coated and joined by polypyrrole, both showing the central cavity and amorphous polymer layer.[44] (D) Salt spray test result (480 h) for polypyrrole coated mild steel with different PPy loading. From left to right: 4, 6, 8 wt%. No trace of corrosion and degradation could be observed for the coated material, indicating significant enhance anti-corrosion properties.[45]

However, polypyrrole has also been proved as one of the most effective coating materials in the application of anti-corrosion.[45] Unlike the conventional anti-corrosion coating materials, polypyrrole coating could achieve multiple protecting effects within a single coating layer which have substantially enhanced protecting functions compare to the others.[46] It's believed that the

polypyrrole coating could induce the formation of an electric field over the substrate which restricts the electron transfer process occurring on the substrate's surface; moreover, the polypyrrole coating is also able to block the substrate from the surrounding environment, especially the case for air and moisture, which would be the major factors that cause corrosion.[46] There are also some evidences that the mechanical properties of the substrate could be improved considerably by the rigid, good adhered polypyrrole coating, with the extent of improvement could be varying by the coating thickness and smoothness.[47]

Chapter 3

Synthesis of Polypyrrole Coated Copper Nanowires

3.1. Introduction

As described previously, copper nanowires could have great potential as sensory materials due to their intrinsic high electrochemical activity and unique open inter-connected network morphology.[31] However, the main drawback for copper nanowires also lies in the relative weak environmental stability originating from the high reactivity of the bulk copper.[19] It's widely recognized that copper nanowires are very susceptible to oxidation in air with a rapid transformation of its surface lattice from single crystal Cu to Cu_2O.[19] When being applied in solution or moisture condition, the oxidation degradation of the Cu lattice would become much faster and eventually the CuO lattice would substitute the Cu lattice to a considerable extent.[19,29] However, the transformation of Cu lattice to either Cu_2O or CuO lattice is energetically irreversible and it normally deteriorates the electrochemical activity of the copper nanowires permanently. Therefore, in order to achieve stable application properties on the copper nanowires, it's necessary to protect them from the surrounding environment, especially from air and aqueous droplets, to avoid irreversible oxidation degradation of the lattice structure. Polypyrrole coating seems to be a promising route to accomplish this task, based on its high protecting performance, good stability, and ease of implementation.[45] It's speculated that

when being coated with polypyrrole, the environmental stability of the copper nanowire beneath could be enhanced substantially; distinct electrochemical properties could also be expected from the interfacial charge transfer interaction between the conducting coating material and substrate.

3.2. Materials Used and Synthetic Methods

The chemicals used in the synthesis include pyrrole (C_4H_5N, Alfa Aesar, 98%), anhydrous copper (II) chloride ($CuCl_2$, Alfa Aesar, 98%), sodium hydroxide (NaOH, Spectrum, 98%), hydrazine monohydrate ($N_2H_4.H2O$, Alfa Aesar, 98%), acetone (C_3H_6O, Alfa Aesar, 98%), and de-ionized water.

In a typical synthesis process, 1.0 mL of 0.1M $CuCl_2$ was slowly added into 30 mL of 7M NaOH solution under magnetic stirring. 10 minutes' stirring was allowed to obtain a homogeneous blue solution. Afterwards, 0.5 mL of pyrrole was injected into the solution in a slow manner, the color of the solution turned from deep blue to yellowish brown rapidly after the pyrrole injection. Then the mixture solution was allowed to incubate for 30 minutes in order to achieve thorough interaction of the reactants within. 0.01 mL of hydrazine monohydrate was slowly added into the mixture solution after the incubation, at the same time the reaction temperature was risen to 60 $^{\circ}C$ at the rate of 1.5 $^{\circ}C$ /min. The mixture solution was then allowed to undergo the thermal reduction process for 1 hour at 60 $^{\circ}C$, and the color of the reaction solution would gradually transform from dark brown to light yellow, indicating the completion of reaction. The separation of the as-synthesized polypyrrole coated copper nanowire from the solution residues and by-products is also very important. In a typical process, the mixture solution was transferred to a centrifuge tube after reaction, which was then centrifuged at 4000 rpm for 10 minutes in order to separate the solid products from the solution. Afterwards, the as-

obtained solid products were redispersed in 20 mL de-ionized water and centrifuge at 2000 rpm for 20 minutes. The supernatant was poured out in order to remove the particle-like products from the copper nanowires. This centrifuge-redispersed process could be repeated for several times in order to achieve thoroughly removal of the particle products. Eventually the remaining solid products were subject to re-dispersed in 20 mL acetone and centrifuge at 4000 rpm for 10 minutes to remove any solvent residues or pyrrole monomers. The as-obtained solid product could either be stored in 0.25% hydrazine aqueous solution or air-dried at ambient condition.

Chapter 4

Characterization of Polypyrrole Coated Copper Nanowires

4.1. Electron Microscopy (EM) Characterization

The morphological and size information of the as-synthesized polypyrrole coated copper nanowires could be readily obtained with the electron microscopy characterization methods. As a result, scanning electron microscopy (SEM) and high resolution transmission electron microscopy (HRTEM) have been utilized to provide a detail insight about the shape and size characteristics of the as-synthesized polypyrrole coated copper nanowire in nanoscale.

4.1.1. Sample Preparation for SEM & HRTEM

In a typical process, samples for SEM characterization were prepared by dispersing 5 mg of the as-synthesized polypyrrole coated copper nanowire in 5 mL ethanol by bath sonication. Approximate 20 minutes' sonication was required to obtain a relative homogeneous dispersion. Afterwards, the as-obtained dispersion was dropped casted onto a silicon wafer which was attached to the aluminum sample mount by carbon paste. The droplet was then allowed to air-dry on the silicon wafer before subjecting to SEM characterization.

The sample preparation for HRTEM is similar to the ones of SEM. Typically 3 mg of the as-synthesized polypyrrole coated copper nanowire were dispersed in 1 mL ethanol through 20

minutes' bath sonication. Thereafter the dispersion was drop casted onto the copper grid and air-dried for HRTEM characterization.

4.1.2. Results of SEM Characterization

The resulting morphologies of the as-synthesized polypyrrole coated copper nanowires from SEM could be seen from Figure 7. As one could seen, the nanowires shown in Figure 7 has a diameter around 350 nm and lengths reaches up to 10 μm, which shows an aspect ratio around 28. The surfaces of the as-obtained nanowires are roughly coated with an amorphous layer, which could be ascribed to the polypyrrole coating. The copper nanowires are randomly distribu-

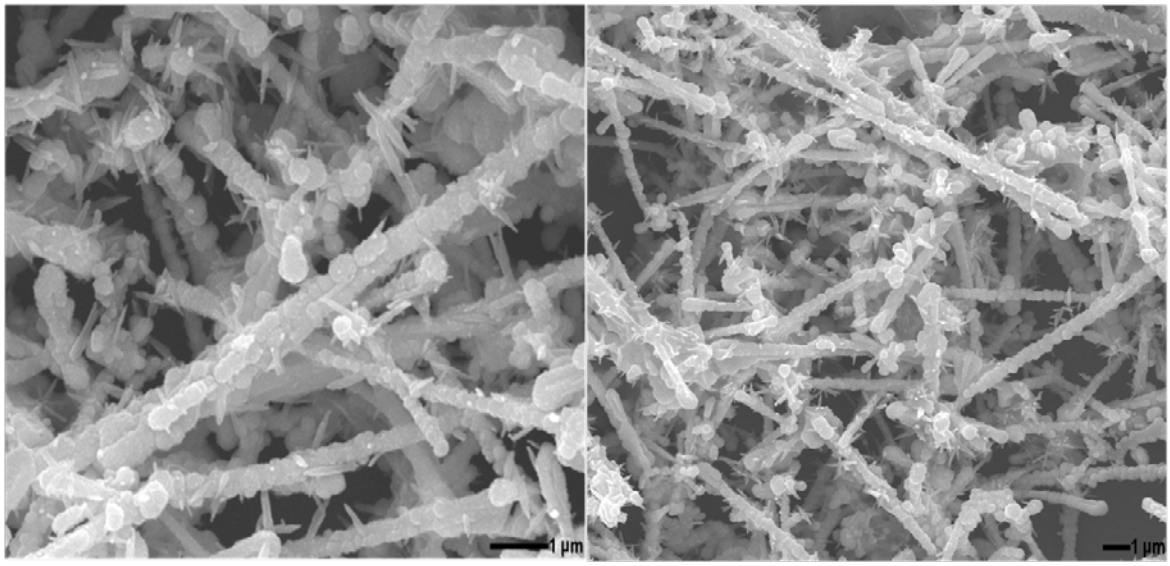

Figure 7. SEM image of the as-synthesized polypyrrole coated copper nanowires

ted over the supporting silicon wafer and intermeshed with each other, forming an extensive open interconnected network with high nanowire density.

4.1.3. Results of HRTEM Characterization

The HRTEM image of the as-synthesized polypyrrole coated copper nanowires could be shown as Figure 8, which was taken from the area near the surface of the nanowire. It could be

clearly observed from Figure 8 that copper lattices with fringe spacing of 2.1 Å are uniformly arranged along the [110] direction with no other lattice configuration could be observed. And the 2.1 Å fringe space could be attributed to the {111} reflection of face-centered cubic (*fcc*) Cu.

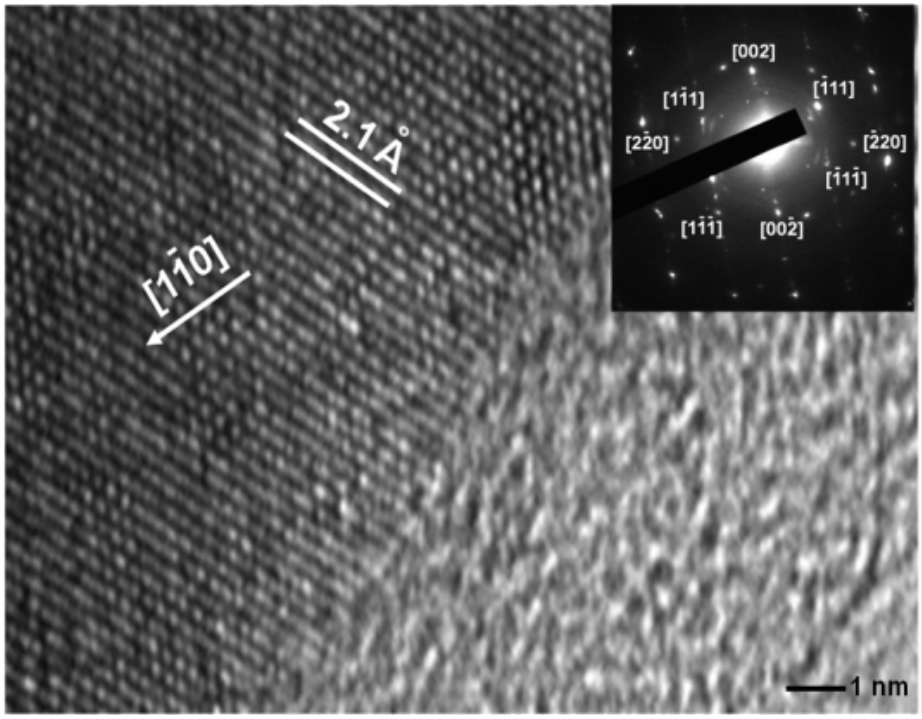

Figure 8. HRTEM image of the as-synthesized polypyrrole coated copper nanowires. Inset shows the SAED pattern of nanowires.

These observations evidence the as-obtained copper nanowires are single crystalline face-centered cubic (*fcc*) Cu crystals.[29] From the HRTEM image it's also clear to observe the existence of an amorphous coating layer on top of the Cu crystal lattices. This amorphous layer extends up to 5-6 nanometers with featureless structures under the HRTEM observation, which could be attributed to the formation and adhesion of polypyrrole coating on the surface of the copper nanowires. Inset of Figure 8 shows the selected area electron diffraction (SAED) pattern of the as-obtained copper nanowire, it could be inferred from this pattern that the copper nanowire is a piece of single crystal growing along the {110} direction with its {111} facets exposed on the surface.[29] Therefore, based on the HRTEM observation, it could be concluded

that single crystalline copper nanowires with a polypyrrole coating layer of approximate 5-6 nanometers could be readily obtained in a one-pot manner, which could be very intriguing as enhanced environmental stability and electrochemical activity are expecting from the incorporation of these two distinct materials.

4.2. X-ray Diffractometry (XRD) Characterization

The crystallographic characteristics of the as-synthesized polypyrrole coated copper nanowires are subject to analyze with the X-ray diffractometry (XRD) technique. The as-obtained XRD pattern could be shown as Figure 9.

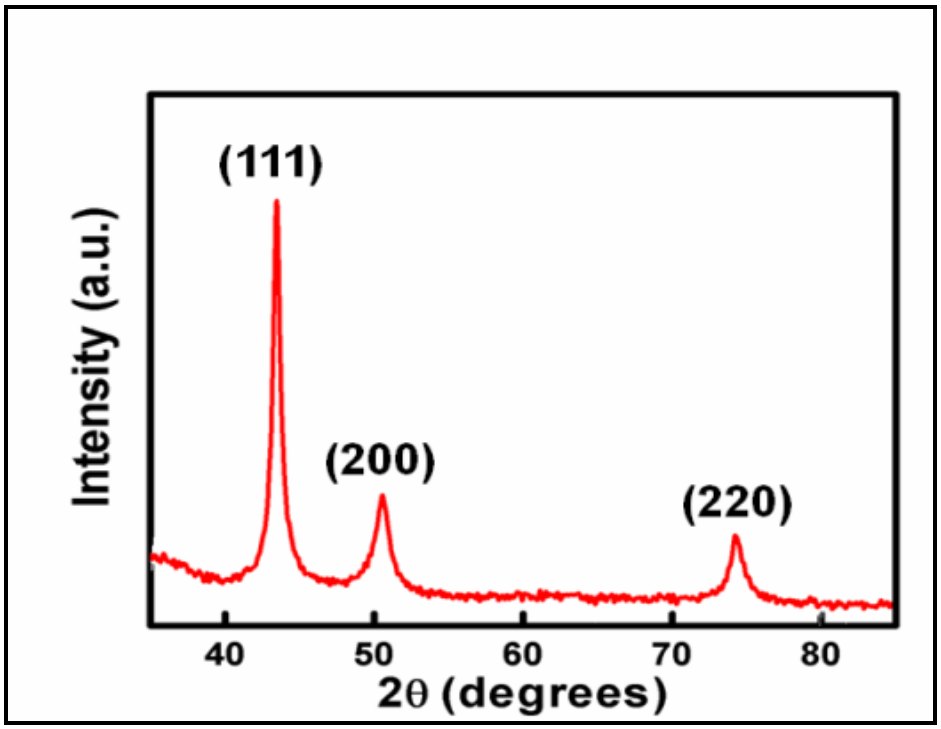

. ***Figure 9.*** XRD pattern of the as-synthesized polypyrrole coated copper nanowires

Three diffraction peaks at $2\theta = 43.2^{\circ}, 50.4^{\circ}, 74.1^{\circ}$ could be observed clearly from the XRD pattern, which could be indexed to the diffraction of {111}, {200}, and {220} crystal planes of face-centered cubic (*fcc*) Cu, respectively. The lattice constant of this crystalline phase could be calculated from the XRD pattern as $a = 3.614\,\text{Å}$, which is very close to the standard value of

$a = 3.615\,\text{Å}$ (JCPDS 4-836). No characteristic diffraction peak around $2\theta = 36.5^{\circ}$ corresponding to the formation of surface oxidized Cu_2O layer could be seen from the XRD pattern of the as-synthesized polypyrrole coated copper nanowires, which normally exist with the copper nano-materials after they have been synthesized for a few hours.[19,29] Nevertheless, the formation of a thin Cu_2O layer on the surface of copper nanomaterials could be attributed to the intrinsic high surface energy and reactivity of the nanoscale copper, which is generally unfavorable for it would slowly convert the whole copper crystal to its oxidized form in a "top-down" manner. However, the absence of Cu_2O peak for polypyrrole coated copper nanowires inevitably indicates the extraordinary surface protection ability of the polypyrrole coating layer towards the copper nanocrystal underneath, which is very favorable in pertaining the electrochemical activity of the copper nanocrystal for long-term usage.

4.3. Energy Dispersive X-ray Spectroscopy (EDX) Characterization

The as-obtained polypyrrole coated copper nanowires were also subject to be analyzed by EDX, in order to reveal their elemental composition and atomic distribution. The resulting EDX spectrum could be shown as Figure 4. Based on the spectroscopic observation of Figure 10, the elemental composition of the as-obtained polypyrrole coated copper nanowires could be unambiguously indexed to C^{12}, N^{14}, O^{16}, and Cu^{64}, whereas the Au^{197} counts are resulting from the sputter gold coating during the sample preparation stage. However, the existence of C^{12}, N^{14}, and O^{16} elements within the as-prepared sample could be attributed to the polypyrrole coating on the surface of the copper nanowires, and the O^{16} element is possibly resulting from the adsorbed atomic oxygen or oxidation defects within the polypyrrole chains.[48] The relative abundance of

Cu^{64} compared with other elements shown in the EDX spectrum also reveals that the nanowires are majorly composed of copper atoms, indicating its characteristic nature as copper nanowires.

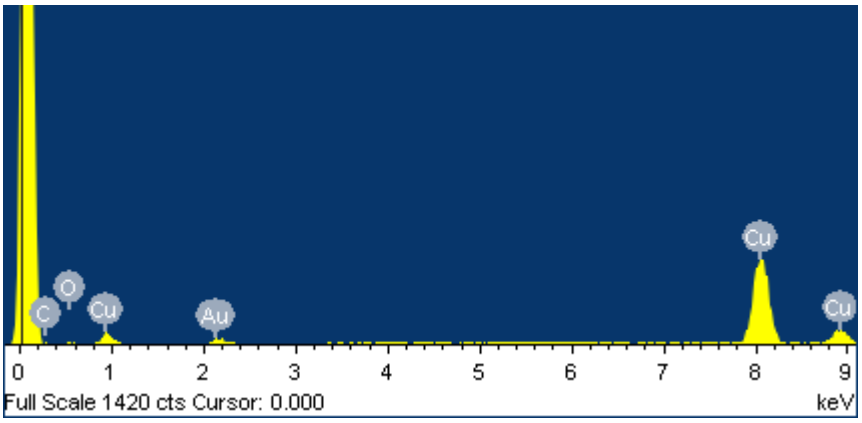

Figure 10. EDX spectrum of the polypyrrole coated copper nanowires

Table 1. Elemental analysis results of the polypyrrole coated copper nanowires from EDX

Elements	Weight (%)	Atomic (%)
C	133.11	41.49
N	93.54	25.00
O	21.26	4.98
Cu	484.14	28.53
Total	732.05	100

The elemental analysis result of the polypyrrole coated copper nanowires based on the EDX spectrum could be shown as Table 1. From Table 1 we could see the weight composition and atomic composition of the as-obtained polypyrrole coated copper nanowires. It could be seen from the atomic composition that the atomic portion of C^{12} is much higher than that of Cu^{64}, and the portion of N^{14} is comparable to Cu^{64}. This phenomenon reveals that the near surface area of the as-obtained polypyrrole coated copper nanowires is majorly covered by polypyrrole, which makes the limiting accessibility of the copper nanowires underneath for the electron beam which incites the X-ray signal for EDX mapping. On the other hand, the small oxygen composition indicates a rather moderate oxidation level of the polypyrrole coating layer.

4.4. Fourier Transform Infrared Spectroscopy (FT-IR) Characterization

FT-IR spectroscopy was also utilized to characterize the surface chemical composition of the as-synthesized polypyrrole coated copper nanowires. The resulting FT-IR spectrum could be shown as Figure 11. Multiple peaks inferring the chemical structure and surface composition of the as-obtained polypyrrole coated copper nanowires could be observed within the FT-IR spectrum. However, the IR spectroscopic pattern of polypyrrole coated copper nanowires resembles the one of pure polypyrrole. As the obvious bands located at 3100~2800 cm^{-1} and 800~600 cm^{-1} could be assigned to the N-H/C-H stretching modes and C-H out-of-plane bending mode of polypyrrole, respectively.[49,50] On the other hand, two intense peaks located at 1270 and 1110 cm^{-1} could be ascribed to the C-H ring in-plane bending mode whereas another peak at 1320 cm^{-1} could be assigned to the C-N stretching modes.[50] After all, one intense peak located at 1690 cm^{-1} could be assigned to the C=O stretching mode, which reveals the existence of pyrrolidinone segments within the polypyrrole backbone.[51]

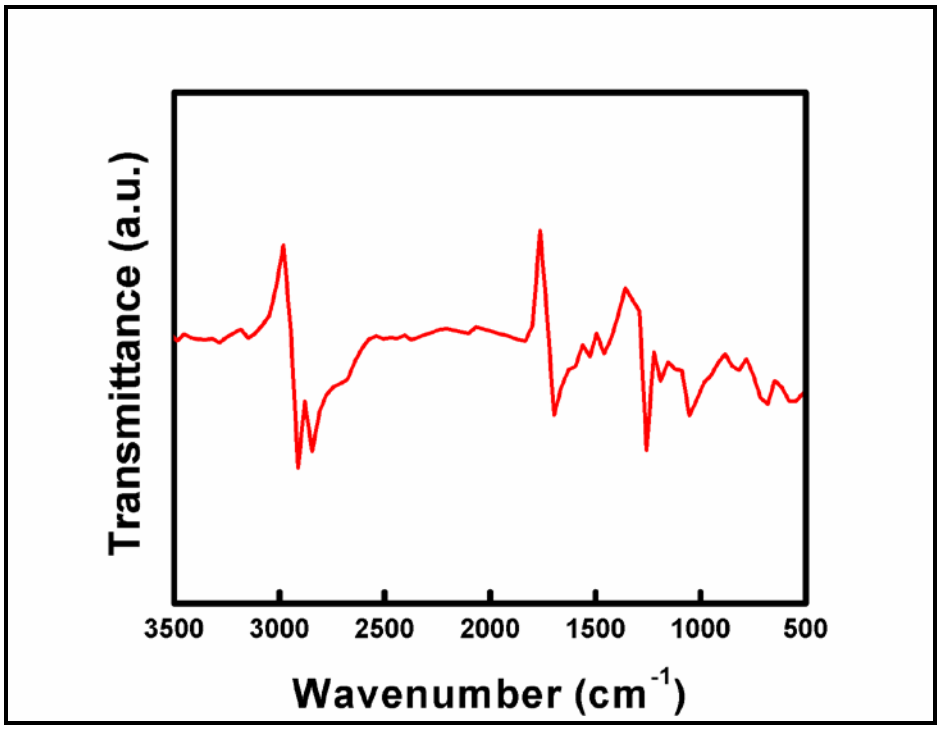

Figure 11. FT-IR spectrum of the polypyrrole coated copper nanowires

The as-obtained FT-IR spectrum thus inevitably reveals the existence of polypyrrole coating on the surface of the copper nanowires. For the peak shapes and positions of their FT-IR spectrum are coincided with each other. The polypyrrole coating thus changes the surface spectroscopic characteristics of the copper nanowires to a significant extent, for no IR characteristic peak could be observed for the pure Cu materials.[52] A spectroscopic comparison among the pure polypyrrole, polypyrrole coated copper nanowires, and copper particles synthesized without the addition of pyrrole using the proposed synthetic process could be presented in Figure 12.

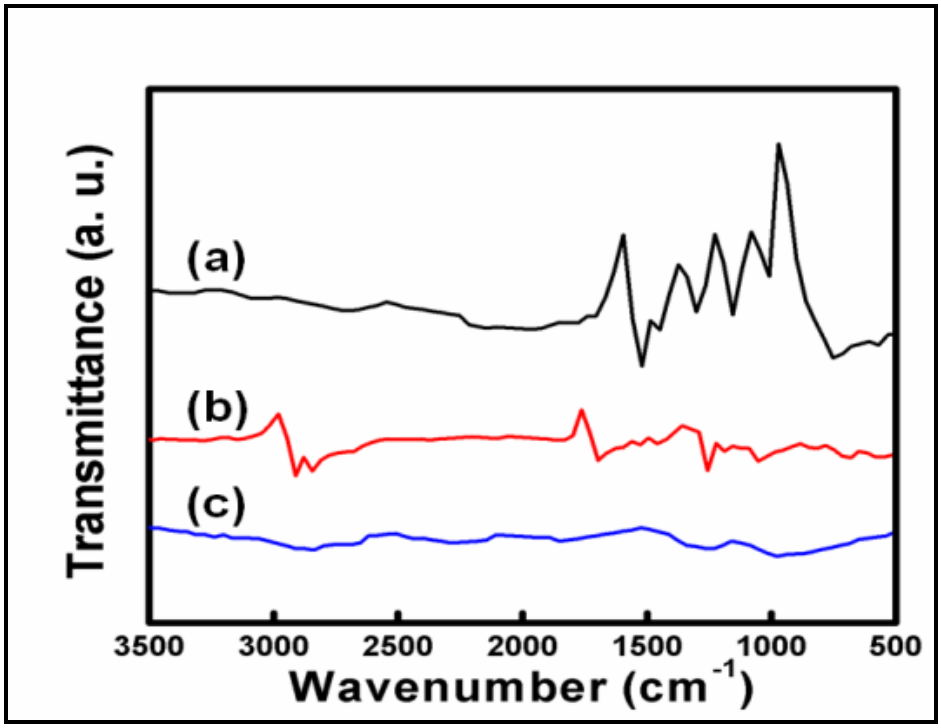

Figure 12. FT-IR spectrum of (a) pure polypyrrole, (b) polypyrrole coated copper nanowires, and (c) copper particles synthesized without the addition of pyrrole.

4.5. UV-Vis Spectroscopy (UV) and Thermal Gravimetric Analysis (TGA) Characterization

Characteristic electronic states and thermal behaviors of the polypyrrole coated copper nanowires are analyzed by the techniques of UV and TGA. The resulting UV spectrum and

TGA thermogram could be shown as Figure 13 and Figure 14, respectively. From the UV spectrum a board absorption band located between 550 and 800 nm could be clearly observed. The formation of this board band could be possibly assigned to the synergistic interaction of two absorption phenomena. One is the surface plasmon resonance of the copper nanowires, which has the characteristic narrow, sharp absorption peak around 590 nm;[53] the other is the polaron excitation band of polypyrrole, which would exhibit a board, flat absorption band starting from around 600 nm and extends to near IR region, indicating the localized/delocalized polaron distribution of the polymer chains.[54]

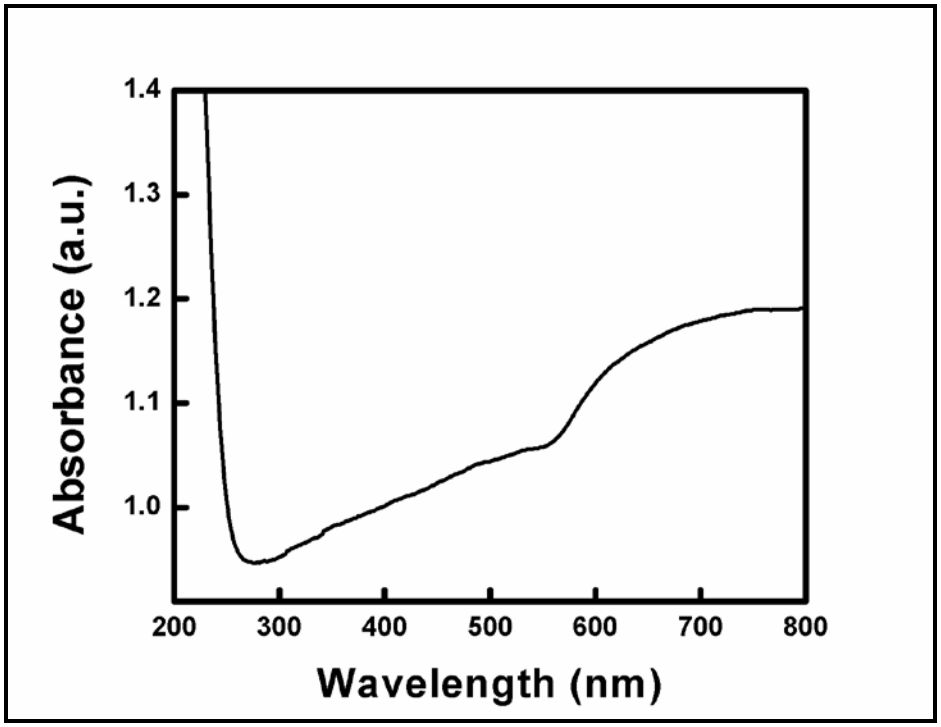

Figure 13. UV-Vis spectrum of the as-synthesized polypyrrole coated copper nanowires

However, the TGA graph regarding the thermal properties of the as-synthesized polypyrrole coated copper nanowires, pure polypyrrole, and cut pieces of copper foil was shown in Figure 14. It could be observed that under the condition of elevating temperature from 200 to 800$^{\circ}C$ and air flow, polypyrrole was readily subject to thermal degradation and exhibited a continuous weight

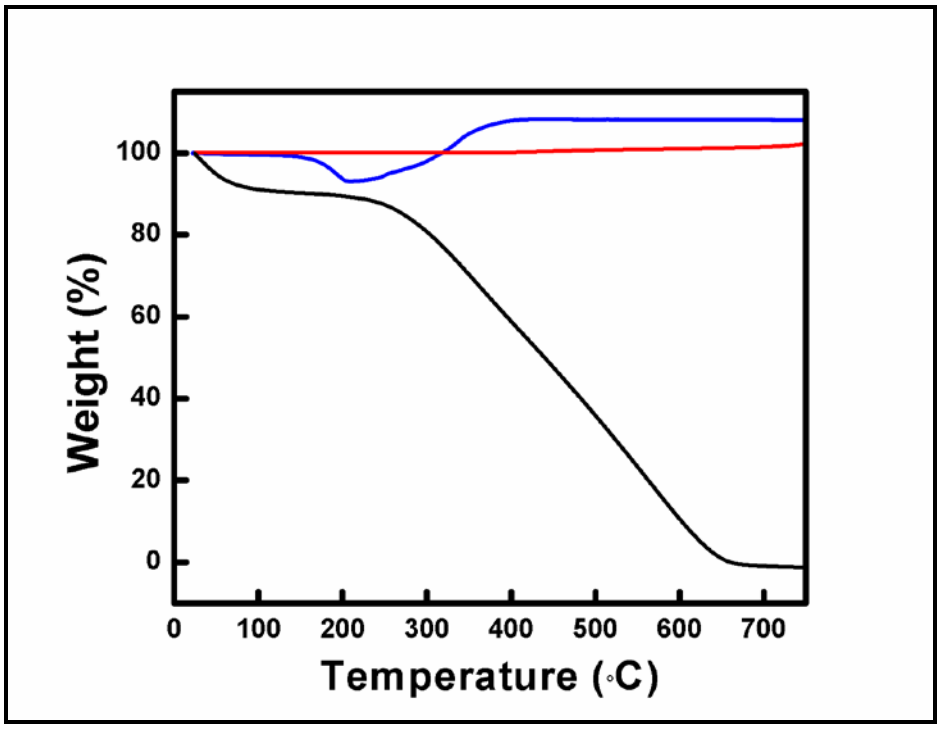

Figure 14. TGA thermograms of pure pyrrole (black), cut copper foil (red), and polypyrrole coated copper nanowire (blue).

loss toward almost 100%. On the other hand, there is no observable weight loss for the cut copper foil under the experiment condition, indicating the significant thermal degradation resistance of the copper materials. To consider the case of polypyrrole coated copper nanowires, a clear down wave of the thermogram below $200^{\circ}C$ could be readily observed, and a weight loss around 7% was obtained. This weight loss of the material could be possibly attributed to the degradation of the polypyrrole coating layer, as the thermal stability of polypyrrole remains poor within this range whereas the copper substrate underneath behaves relative high thermal stability under this range. Nevertheless, a weight gain of 15% could be observed for the polypyrrole coated copper nanowires starting from the temperature around $208^{\circ}C$, and end at around $430^{\circ}C$. This significant weight gain could be ascribed to the surface oxide formation process of the copper nanowires. As their surface coating layer of polypyrrole continuous degraded and

exposed the copper substrate to surface oxidation in air. It could be inferred from the TGA thermograms that copper nanowires were more susceptible to air oxidation compared to the bulk copper foil, indicating the lowering thermal stability upon transforming the bulk copper material to nanoscale. However, this phenomenon could be majorly ascribed to the size-effect deriving from the nanoscale copper wires, which is thermodynamically unfavorable and easily undergo phase transitions upon applied energy.[19]

Chapter 5

Formation Mechanism Study of the Polypyrrole Coated Copper Nanowire

5.1. UV-Vis Spectroscopy Monitoring of the Synthetic Process

UV-Vis spectroscopy (UV) is one of the most widely used methods to study the formation mechanism of various kinds of substances. However, information regarding the electronic state and molecular structures of the substances could be readily obtained through UV spectroscopy, as a result of the characteristic absorption bands of different molecules and the same molecules with different features (oxidation state, configuration, size, etc.). Nonetheless, UV spectroscopy is widely recognized as one of the most effective methods to investigate the formation mechanism of organic compounds, metal complexes, and metallic nanocrystals, as the changes of electronic state, complex composition, as well as the shape/size of the intermediates and products during the synthetic process could be readily reflected by the corresponding adsorption spectral change.[55] Here we utilized the UV spectroscopy to investigate the formation mechanism of the as-synthesized polypyrrole coated copper nanowire, as significant changes of the complex composition and electron transfer process could be expected during the synthetic process.

5.1.1. Experimental Procedures for the UV measurement

SHIMADZU UV-2450 spectrophotometer was utilized to perform the UV measurements of the reaction solutions in order to obtain the information regarding the spectral changes throughout the synthetic process of the polypyrrole coated copper nanowire. Typically 0.3 mL of the reaction solution was extracted from the bulk using a syringe every 10 minutes during a standard synthetic process. Thereafter the extraction was placed in a 20 mL distillation vial and diluted 30 times with de-ionized water. The diluted solution was then subject to the UV measurement using quartz cuvette with an optical length of 1 cm.

5.1.2. Results of the UV measurement

The resulting UV spectra regarding the whole synthetic process is shown as Figure 15 and 16. Figure 15 represents the spectral changes from 200 to 325 nm whereas Figure 16 represents the enlarged view of spectral changes from 325 to 525 nm. However, it was believed that pyrrole would coordinate with the cupric ions even in the highly alkali solution (7M NaOH), as pyrrole has possessed very high pK_a and it is not likely to dissociate in this highly alkali solution.[56] The coordination of pyrrole to the cupric ions could be evident by the emergence of the ligand-to-metal charge transfer band (LMCT) around 415 nm (Figure 16) after the addition of pyrrole into the reaction solution. The emergence of this band, however, could be possibly attributed to the π(pyrrole)-Cu(II) LMCT.[57] On the other hand, upon addition of pyrrole, the intensity of the main band at 235 nm was also enhanced substantially (Figure 15), which indicated the complexation of pyrrole towards the cupric ions. And the enhancement in intensity of the main band could be possibly attributed to the σ(N)-Cu(II) LMCT of the as-formed complexes, which is blue shift compared to that of aliphatic amines.[58]

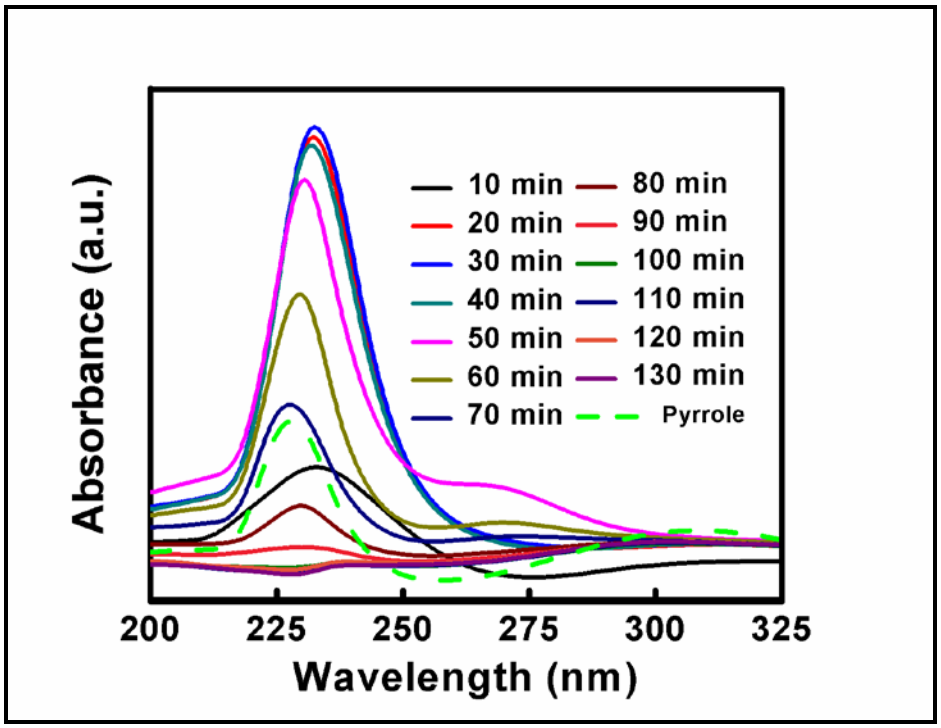

Figure 15. UV spectral changes for the whole synthetic process of polypyrrole coated copper nanowire from 200 nm to 325 nm. The individual spectrum was taken in 10 minutes' interval from the reaction solution.

However, upon the addition of hydrazine into the reaction solution to trigger the thermal reduction process, the structures of the complexes were visibly disrupted as reflected by the spectral changes of the UV spectra. Nonetheless, the lowering intensity of the main band at 235 nm along with the disappearance of the LMCT band at 415 nm together reveal the weakening interaction between the pyrrole ligand and central cupric ion. A new shoulder band also emerged around 273 nm, which could be possibly ascribed to the vibrational structures of the intense band at 235 nm.[59] However, such spectral changes are expectable as hydrazine continuously reducing Cu^{2+} to Cu^{0} after its addition.[60] On the other hand, the amount of Cu^{2+}-pyrrole complexes decreases substantially as the concentration of the cupric ion decreases, resulting in diminishing intensity of the main band at 235 nm. It could be observed in Figure 15 that the main band at 235 nm eventually stabilized at relative low intensity which corresponding to the completion of the

synthetic process. Interestingly, this intensity value is lower than either the one of pure pyrrole or the original Cu^{2+} solution, and no characteristic band around 220 nm for pyrrole is shown.[61] This phenomenon thus strongly suggests the incorporation of pyrrole molecules into the final copper product, presumably in the form of polypyrrole.

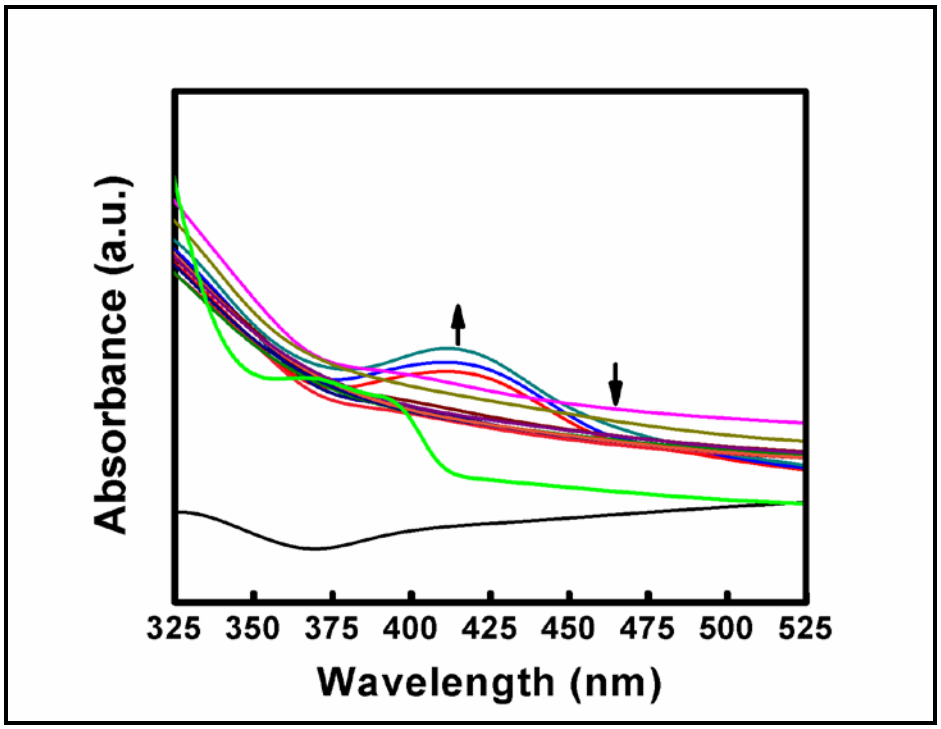

Figure 16. UV spectral changes for the whole synthetic process of polypyrrole coated copper nanowire from 325 to 525 nm. The individual spectrum was taken in 10 minutes' interval from the reaction solution. And the Y-axis was 16 times magnified as compared with the one shown in Figure 15.

5.2. Open Circuit Potential Monitoring of the Synthetic Process

Open circuit potential (OCP) measurement was also implemented to investigate the formation mechanism of polypyrrole coated copper nanowire. Differing from other characterization methods, the OCP measurement could provide the information regarding the overall oxidation and reduction power of the species within the reaction solution, and the reaction kinetic could also be reflected through the direction and extent of the potential change during the synthetic process.[62] As a result, in order to give a deeper understanding about the

kinetic and redox directions during the synthetic process, OCP measurement was applied to monitor the potential change of the reaction solution throughout the synthetic process.

5.2.1. Experimental Procedures for the OCP measurement

The OCP profile of the reaction solution was monitored by the Arbin instruments' BT 2000 testing system during the synthetic process. A conventional three electrode cell configuration was installed and connected to the testing system to implement the OCP measurement. A platinum foil was utilized as the working electrode while a platinum wire was used as the counter and saturated calomel electrode (SEC) as the reference. The three electrode cell was immersed into the reaction solution at the very beginning before the addition of any reactants. Thereafter 10 minutes' interval was allowed before the addition of 0.1 M $CuCl_2$ into the reaction solution in order to stabilize the potential of the electrode cell. A standard synthetic process (with the addition of pyrrole) and its control (without the addition of pyrrole) were then implemented on the reaction solution; whereas the potential of the reaction solution was monitored simultaneously throughout the synthetic process by the electrode cell.

5.2.2. Results of the OCP measurement

The as-obtained OCP profile corresponding to the whole synthetic process could be shown as Figure 17. It could be seen from Figure 17 that the addition of $CuCl_2$ into the reaction solution results in a clear raise of the potential, indicating the increased oxidation power of the reaction solution according to the Nernst equation. However, upon the addition of pyrrole into the solution, a significant decrease of the potential could be observed, inferring the oxidation power

of the reaction solution was substantially reduced by pyrrole. In other words, pyrrole could possibly lower the oxidation potential of the solution through its redox reaction with cupric ions,

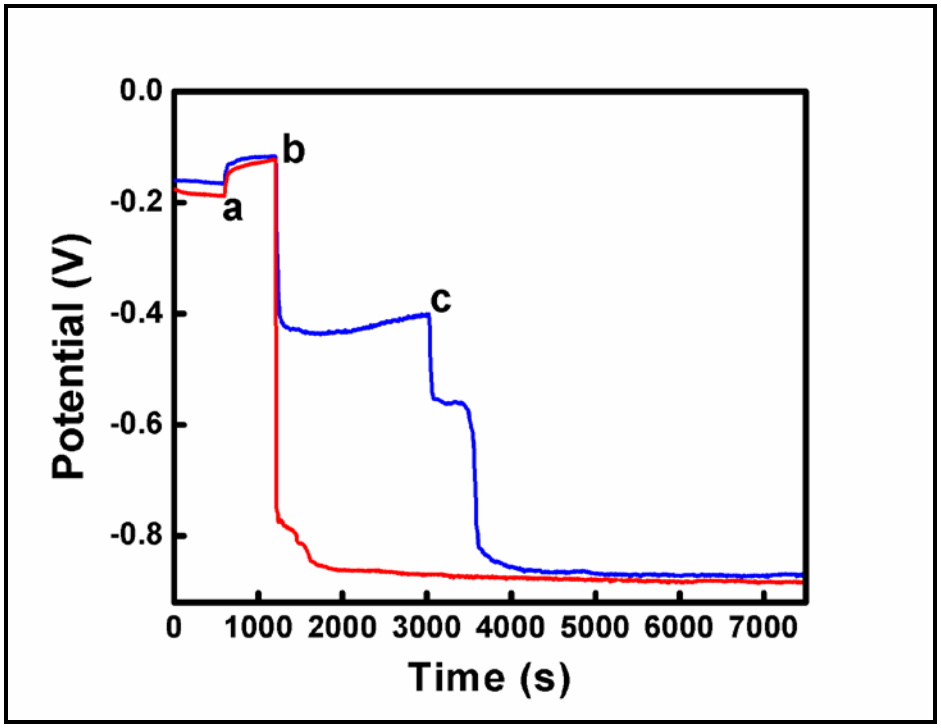

Figure 17. Open circuit profiles corresponding to the whole synthetic process of polypyrrole coated copper nanowire with (blue) and without (red) the addition of pyrrole. Response upon addition of (a) $CuCl_2$; (b) pyrrole (blue) and hydrazine (red); (c) hydrazine could be seen from the profiles.

as it has long been evident that cupric ions could readily oxidize pyrrole.[63] Nonetheless, a slightly raise of the equilibrium potential could be observed within the OCP profile segment of b-c. This phenomenon could be possibly attributed to the formation of polypyrrole with partially oxidized benzoquinone chain segments, which has possessed certain oxidation power and is capable of encapsulating free oxygen in the surrounding environment.[48] Formation of this polypyrrole product could also be evident by the color change of the reaction solution during this stage, as it darkens substantially and the color changes from light blue to dark brown (Figure 18). It's also noteworthy that a visibly step could be observed from the OCP profile of the synthetic process with the addition of pyrrole, whereas only subtle transition curve segment could be obs-

erved according to the case of without adding pyrrole. Nevertheless, this significant step unambiguously indicates the notable interaction between pyrrole and cupric ions within the reaction solution. And it could be ascribed to a complex redox process which involves Cu^{2+}, pyrrole, and hydrazine. Furthermore, relative longer time is required for the reaction solution to reach the ultimate equilibrium potential at -0.86 V in the presence of pyrrole also reveals that the reactivity of Cu^{2+} has been altered via its complexation with pyrrole.[64]

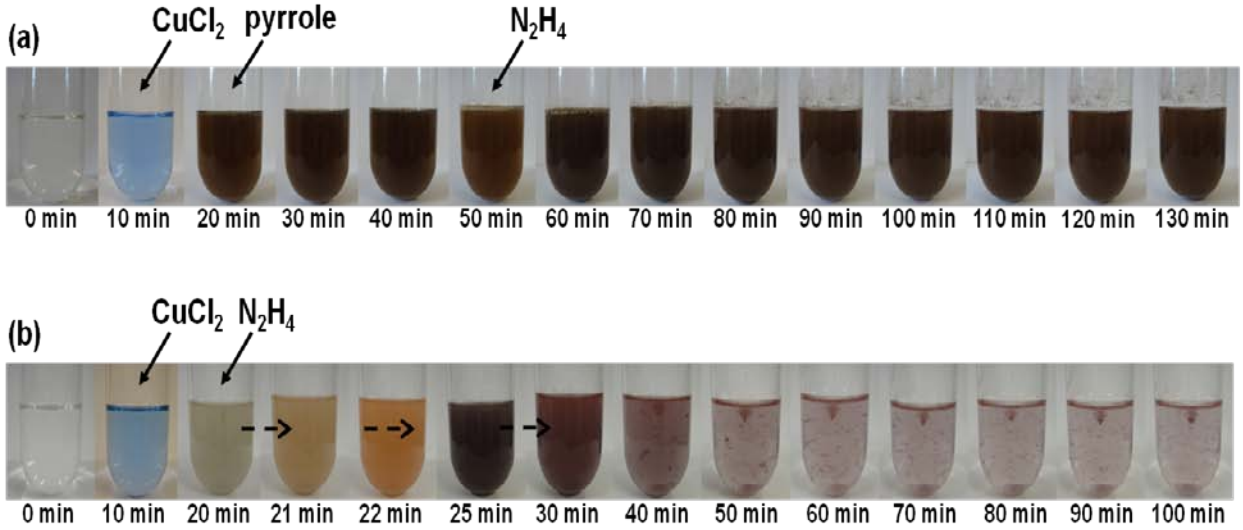

Figure 18. Photographs of the reaction solution for the synthesis of polypyrrole coated copper nanowire with (a) and without (b) the addition of pyrrole.

5.3. Proposed Formation Mechanism for Polypyrrole Coated Copper Nanowire

Based on the results and discussion from the UV and OCP measurements, a brief formation mechanism could be proposed for the polypyrrole coated copper nanowires. In highly concentrated alkali solution, the reactivity of Cu^{2+} was lowered upon its complexation with hydroxyl ions to form alkali cuprates (CuO_2^{2-}).[65] When pyrrole was introduced into this solution, it further coordinated with the cuprates to form complexes with the Cu^{2+} as the metallic centers. Simultaneous oxidation of pyrrole and reduction of Cu^{2+} metallic center would happen within

the complexes via the LMCT excitation, which led to the formation of both pyrrole cationic radicals and Cu^0 atoms. Thereafter the pyrrole radicals would initiate the polymerization of pyrrole through free radical polymerization and the Cu^0 atoms would also assemble into small Cu particles. As these processes proceeded, eventually it would form Cu nanoparticles with polypyrrole capping within the reaction solution. As hydrazine was introduced into the reaction solution, it would then reduce all the existing copper ions into Cu nanoparticles; at the same time the Cu particles with polypyrrole capping would serve as the seeds for the growth of Cu nanowires through the Oswald ripening process.[66] On the other hand, the polymerization of pyrrole would still proceed as the Cu nanowires were growing, and the propagating polymer chains would then adsorb onto the Cu nanowires' surface by the coordination effect of the amine functional groups.[67] Thus it could be concluded that this synergistic crystal growth and polymerization process eventually leads to the formation of Cu nanowires with a thin layer of polypyrrole coating.

Chapter 6

Electrochemical Properties of Polypyrrole Coated Copper Nanowire & Its Application in Sensing Hydrogen Peroxide

6.1. Electrochemical Properties of Polypyrrole Coated Copper Nanowire

The electrochemical properties play an essential role both in evaluating the application performance of polypyrrole coated copper nanowire as chemical sensors and understanding the possible redox mechanism involved between the working electrode and the stimuli. Varying kinds of electrostatic and dynamic methods could be applied to probe the sensory properties of specific electrode materials towards certain kinds of electroactive species, such as potentiometric, amperometric, chemiresistive, and voltammetric methods.[68] However, the potentiometric method has possessed the advantages of high sensitivity, rapidity, simplicity, and non-destructiveness.[69] A polypyrrole coated copper nanowire modified graphite electrode (PPy-CuNW/G) thus fabricated and potentiometric method was utilized to investigate its sensory properties towards hydrogen peroxide. On the other hand, voltammetry has been proved to be one of the most powerful tools to study the mechanisms involved during an electrochemical reaction, as it could provide precise demonstration regarding the characteristics of the electron transfer processes within the electrochemical reaction, e.g. the electron transfer kinetics, reversibility of the electron transfer processes, and the elementary chemical reactions involved.[70]

However, various kinds of voltammetric methods have been developed to give a better understanding about the electrochemical processes, including potential step, linear sweep, and cyclic voltammetry. Among these methods, cyclic voltammetry has been most widely used as it could provide comprehensive demonstration of the electrochemical process both involved in the anodic and cathodic reactions, as well as their relationships.[70] Thus upon investigating the cyclic voltammetry characteristics of certain electrochemical cells, the information regarding the reaction mechanism and electron transfer process could be readily obtained. Thereafter a PPy-CuNW/G electrode was fabricated and the cyclic voltammetry method was utilized to investigate its electrochemical characteristics.

6.2. Cyclic Voltammetry Measurement of Polypyrrole Coated Copper Nanowire

Cyclic voltammetry (CV) measurement was performed on the PPy-CuNW/G electrode to explore the electrochemical characteristics of the PPy-CuNW/G electrode under different solution conditions. It was expected that polypyrrole coated copper nanowires would exhibit novel CV features other than characteristic redox waves of copper materials, as a result of the possible interfacial charge transfer interaction between the conducting polypyrrole coating layer and the copper substrate. The cathodic reaction rate of the electrode would also subject to change due to the polypyrrole coating.

6.2.1. Experimental procedures for CV measurement

The CV measurement was performed on the Arbin instruments' BT 2000 testing system equipped with a conventional three electrode cell installation. A PPy-CuNW/G electrode was utilized as the working electrode while a platinum wire was used as the counter and Ag/AgCl as

the reference. The CV measurement was conducted in either 0.1 M NaOH solution or 10 mM phosphate buffer saline (PBS) solution, respectively. The cyclic potential range was set to be -1.0 V to 0.8 V at a scan rate of 20 mV/s. CV measurement of the PPy-CuNW/G electrode were further conducted in 10 mM PBS solution in the presence of 0.1 mM hydrogen peroxide, in order to evaluate the catalytic activity of the electrode towards the reduction of hydrogen peroxide.

A PPy-CuNW/G electrode was fabricated as follows. A graphite electrode was carefully polished with razor blade, rinsed with de-ionized water and ethanol, and then dried under ambient condition in preparatory to use. Afterwards, a thin layer of colloidal graphite paste coating was applied on the surface of the graphite electrode using brushes. 0.1 mg of polypyrrole coated copper nanowire was carefully weighted and attached to the surface of the graphite electrode through the graphite paste. The modified electrode thus was allowed to dry under ambient conditions for 15 minutes before use.

6.2.2. CV Measurement Results of the PPy-CuNW/G Electrode

CV measurements were conducted for the PPy-CuNW/G electrode both in 0.1 M NaOH solution and 10 mM PBS solution. The as-obtained cyclic voltammogram for the case of 0.1 M NaOH solution could be shown as Figure 19. It was shown that the PPy-CuNW/G electrode exhibited typical voltammetric response corresponding to copper based materials, as compared with the observations within the existing literatures. However, it could be seen from Figure 19 that the anodic peak located at -0.35 V and -0.12 V could be attributed to the formation of Cu(I) and Cu(II) species, respectively. At the same time, the apparent anodic wave with an onset potential around 0.48 V indicated the formation of Cu(III) species.[71] However, during the reverse

cathodic scan, the peaks at 0.6 V, -0.48 V, and -0.9 V could be correspondingly ascribed to the transition of Cu(III)/Cu(II), Cu(II)/Cu(I), and Cu(I)/Cu^0.[71] Therefore, It could be concluded from this voltammogram that the PPy coating layer do not alter the electrochemical properties of the copper nanowires underneath to a significant extent, as typical redox pairs of copper species have been displayed.

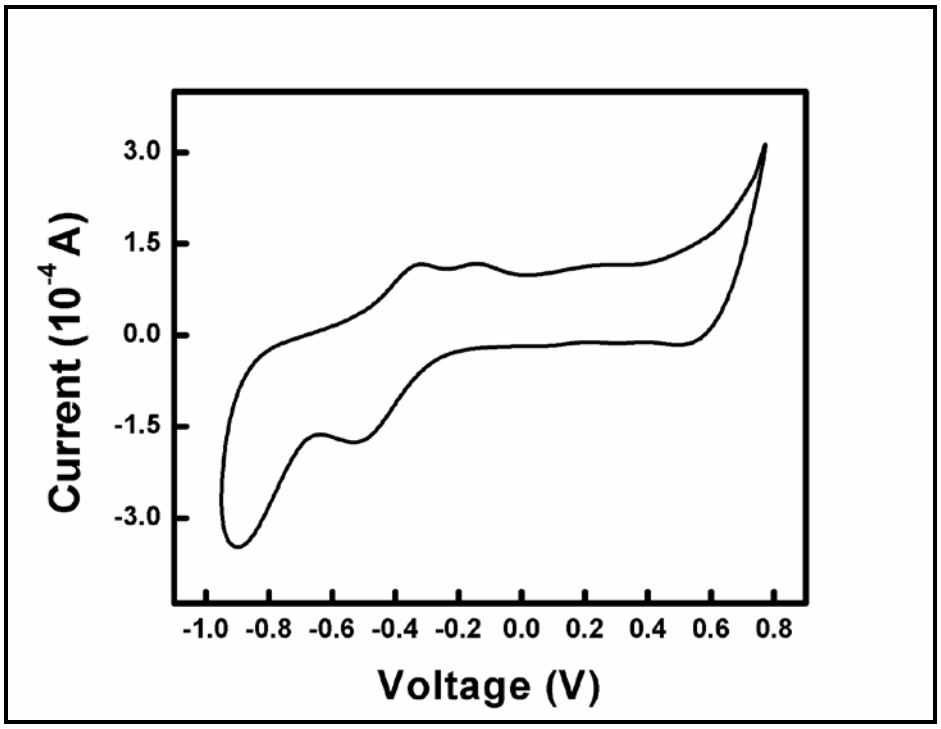

Figure 19. Cyclic voltammogram of the PPy-CuNW/G electrode in 0.1 M NaOH solution. Scan rate: 20 mV/s

However, when the electrolyte solution was changed from 0.1 M NaOH to 10 mM PBS, drastic differences between the as-obtained voltammograms could be observed. It could be seen from the voltammogram of PPy-CuNW/G in 10 mM PBS solution shown in Figure 20 that the peaks and waves corresponding to the phase transitions of copper substrate have been significantly reduced, compared to the case in 0.1 M NaOH solution. Nonetheless, the anodic peak at 0.1 V could be ascribed to the Cu^0/Cu(II) transition whereas the cathodic peak appeared

around 0.45 V could be attributed to the Cu(II)/Cu^0 transition, accordingly.[72] Similar to the case in 0.1 M NaOH solution, the significant anodic wave with an onset potential around 0.48 V could also be attributed to the formation of Cu(III) species.[71] Thereafter it could be inferred from these results that the transitions of Cu^0/Cu(I), and Cu(II)/Cu(I) have been overlapped in the PBS solution for the PPy-CuNW/G electrode, possibly due to the suppression of oxide/hydroxide formation in low pH solution.[71]

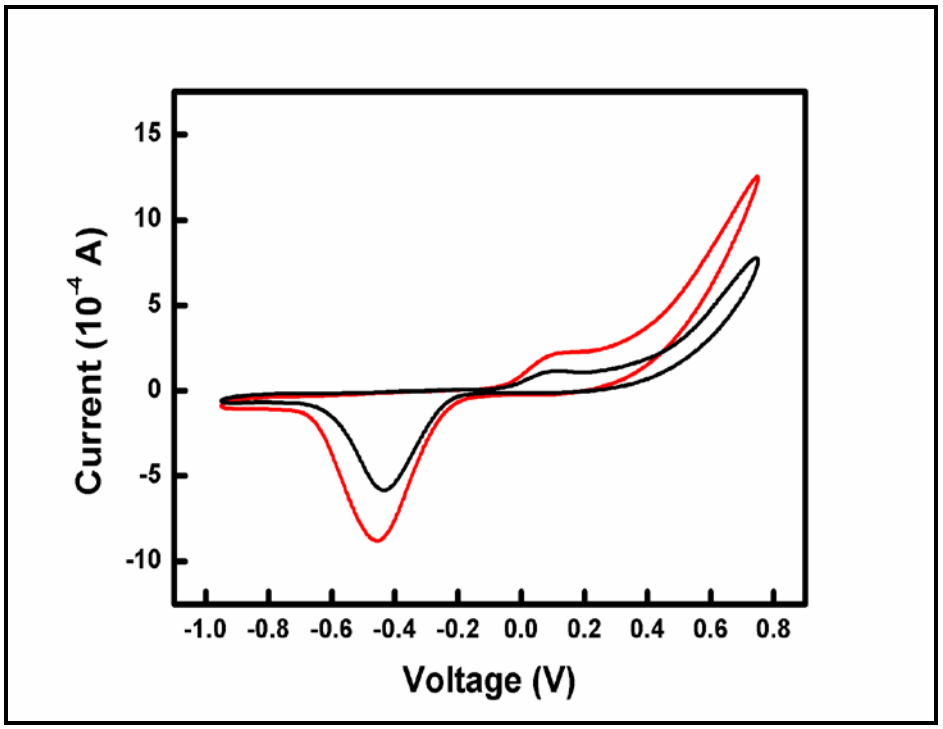

Figure 20. Cyclic voltammograms of the PPy-CuNW/G electrode in 10 mM PBS solution with (red) and without the presence of 0.1 mM H_2O_2.

Upon introducing 0.1 mM hydrogen peroxide into 10 mM PBS solution, an obvious enhancement of current density could be seen from the as-obtained voltammogram of PPy-CuNW/G electrode in Figure 20, especially for the case of the cathodic peak located at -0.45 V. This phenomenon thus unravels the unique electrocatalytic properties of PPy-CuNW towards the reduction of hydrogen peroxide. And the apparent enhancement of the cathodic current could be

ascribed to the improved direct electron transfer process between hydrogen peroxide and PPy-CuNW during cathodic scan.

6.3. Potentiometric Measurement of Polypyrrole Coated Copper Nanowire

Potentiometric measurement was conduct to investigate the sensory properties of polypyrrole coated copper nanowire towards hydrogen peroxide. Potentiometric measurement was chosen due to its high sensitivity, fast response, simplicity, and non-destructiveness.[69] The three electrode configuration was used throughout the potentiometric measurement, while a PPy-CuNW/G electrode was used as the working electrode, a platinum wire as the counter electrode, and an Ag/AgCl electrode as the reference. No current was passed through the circuit of working and counter electrode whereas the potential between them was monitored constantly. It was speculated that the PPy-CuNW/G electrode would give a response of potential change corresponding to the addition of hydrogen peroxide into the testing solution, as a result of the enhancement of cathodic current density in the presence of hydrogen peroxide. The extent of the responding potential change was also believed to be proportional to the concentration of the added hydrogen peroxide.

6.3.1. Experimental Procedures for Potentiometric Measurement

The Arbin instruments' BT 2000 testing system equipped with a conventional three electrode cell was utilized to perform the potentiometric measurement. A PPy-CuNW/G electrode was utilized as the working electrode whereas a platinum wire was used as the counter electrode and Ag/AgCl as the reference. Open circuit condition was applied to the three electrode cell while no current was passed through the cell and the potential difference between the working and reference electrode was monitored continuously. The potentiometric measurement

was conduct in 10 mM PBS solution under constant stirring, and all the measurements were performed after the steady-state potential of the electrode had been achieved. Hydrogen peroxide with different concentration was injected into the stirring PBS solution either in a successive manner with a concentration increment of 0.1 mM or in a single injection manner. The electrode response was taken as the difference between the steady-state and background potential.

6.3.2. Potentiometric Measurement Results of the PPy-CuNW/G Electrode

Typical potentiometric response of PPy-CuNW/G electrode upon successive addition of 0.1 mM H_2O_2 (0.1-1.5 mM) could be shown as Figure 21.

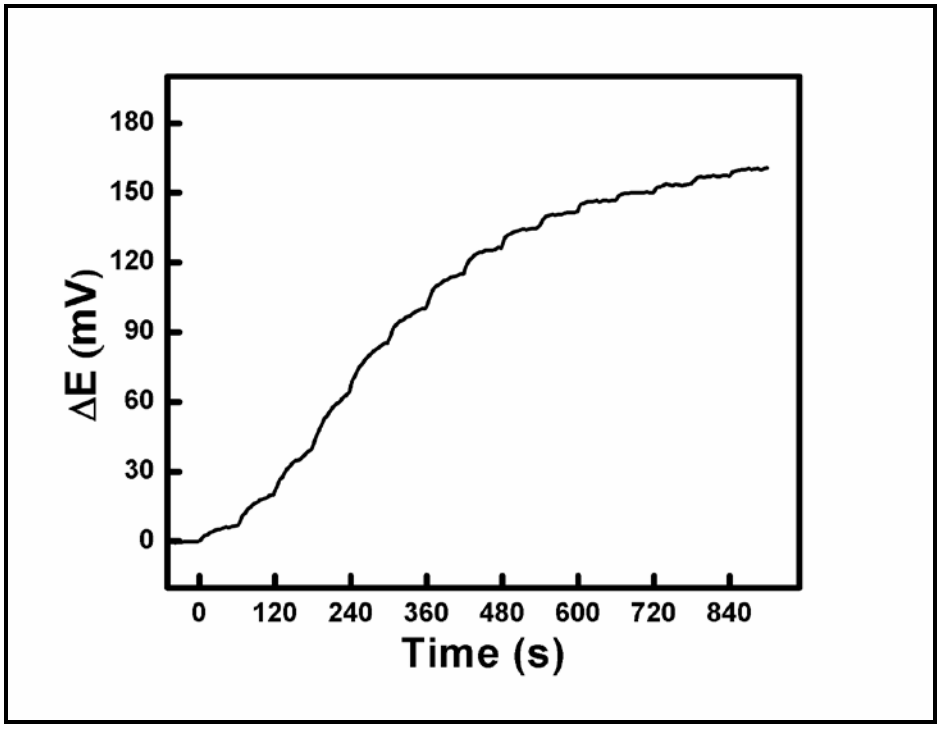

Figure 21. Potentiometric response of a PPy-CuNW/G electrode under successive addition of 0.1 mM H_2O_2 (0.1-1.5 mM) with an increment of 0.1 mM in 10 mM PBS solution.

It could be seen from Figure 21 that the PPy-CuNW/G electrode exhibits relative large potential change corresponding to each addition of H_2O_2, indicating the high sensitivity of the

PPy-CuNW/G electrode towards H_2O_2. On the other hand, the increasing potential for each addition of H_2O_2 reaches its plateau region very quickly, typically within 60s, which otherwise reveals the fast response of the PPy-CuNW/G electrode on H_2O_2. The plateau potentials for each addition of H_2O_2 also exhibit good proportional relationship with the increasing concentrations of the added H_2O_2, proposing the good linear response range of the PPy-CuNW/G electrode corresponding to the detection of H_2O_2.

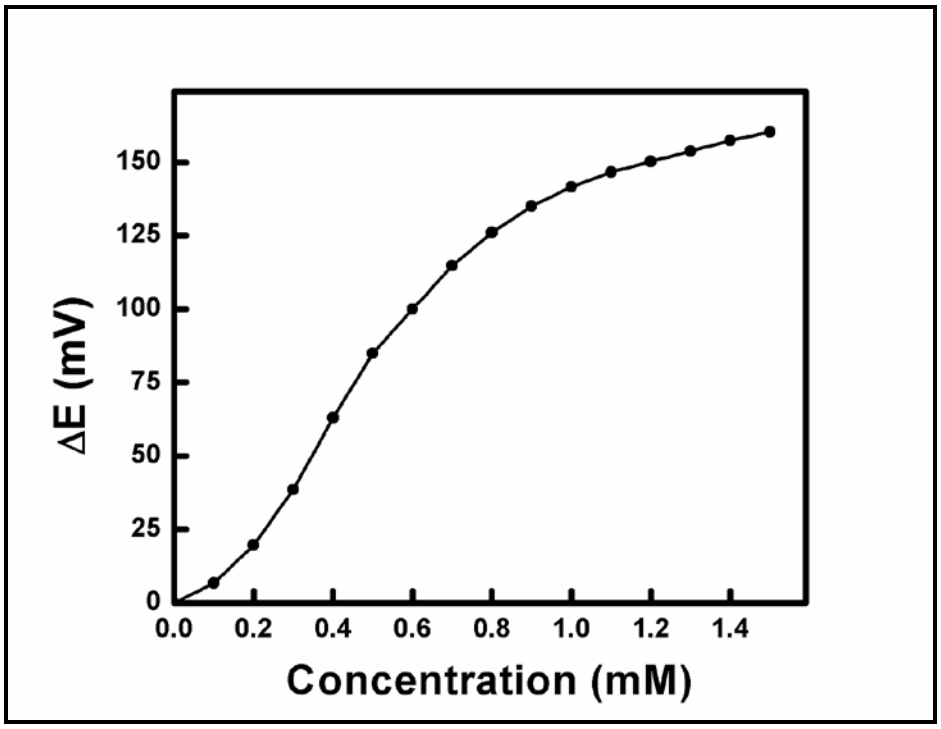

Figure 22. Calibration curve of the PPy-CuNW/G electrode for the detection of H_2O_2 in 10 mM PBS solution.

The calibration curve of the PPy-CuNW/G electrode towards the detection of H_2O_2 could be shown as Figure 22. It was derived from plotting the plateau potential changes shown in Figure 21 against the corresponding H_2O_2 concentrations. However, from the calibration curve it could be observed that the PPy-CuNW/G electrode exhibits linear response range between 0.1-0.8 mM for the detection of H_2O_2 with a sensitivity of 180.65 mV/mM and correlation coefficient (R) of

0.988. This high sensitivity of the PPy-CuNW/G electrode for H_2O_2 could be possibly attributed to the catalytic properties of the PPy-CuNW for the reduction of H_2O_2 through the direct electron transfer process.

The selectivity of the PPy-CuNW/G electrode for the detection of H_2O_2 with the existence of various kinds of interference reagents has also been evaluated. In a typical process, equivalent amount of H_2O_2 and the interference reagent (0.1 mM/0.1 mM) were injected simultaneously into the three electrode cell under open circuit condition. The electrode response according to this injection thus recorded and compared to the electrode response to H_2O_2 (0.1 mM) solely. The relative response of the electrode was taken as the indication of the selectivity for H_2O_2 detection. And it was defined as the percentage of the electrode response with the existence of interference reagent compared to the response without interference reagents, respectively. It could be inferred that the less variation of the relative response from 100%, the higher selectivity could be proposed for the electrode regarding a specific interference reagent. However, the as-obtained distribution of the relative response of PPy-CuNW/G electrode in the presence of interference reagents such as sulfuric acid (SA), nitric acid (NA), ascorbic acid (AA), glucose (Glc), and ethanol (EtOH) could be shown as Figure 23. It could be seen from Figure 23 that the PPy-CuNW/G electrode retains high relative response for H_2O_2 detection with the existence of equivalent amount of interference reagent. For the case of sulfuric acid, nitric acid, ascorbic acid, and ethanol, the electrode retains at least 97% response according to the case of no interference reagent is presented. And the response variation is within the range of $(100 \pm 3)\%$, indicating good selectivity and stability of the electrode response according to the detection of H_2O_2 under these cases. However, when ascorbic acid was utilized as the interference reagent, a significant

decrease in the electrode response could be observed, revealing the notable interference effect of ascorbic acid on the PPy-CuNW/G electrode for the detection of H_2O_2. Nonetheless, this phenomenon could be possibly attributed to the anti-oxidant nature of ascorbic acid and its redox reaction with H_2O_2, which results in a substantial decrease of H_2O_2 concentration in the electrode cell.[73]

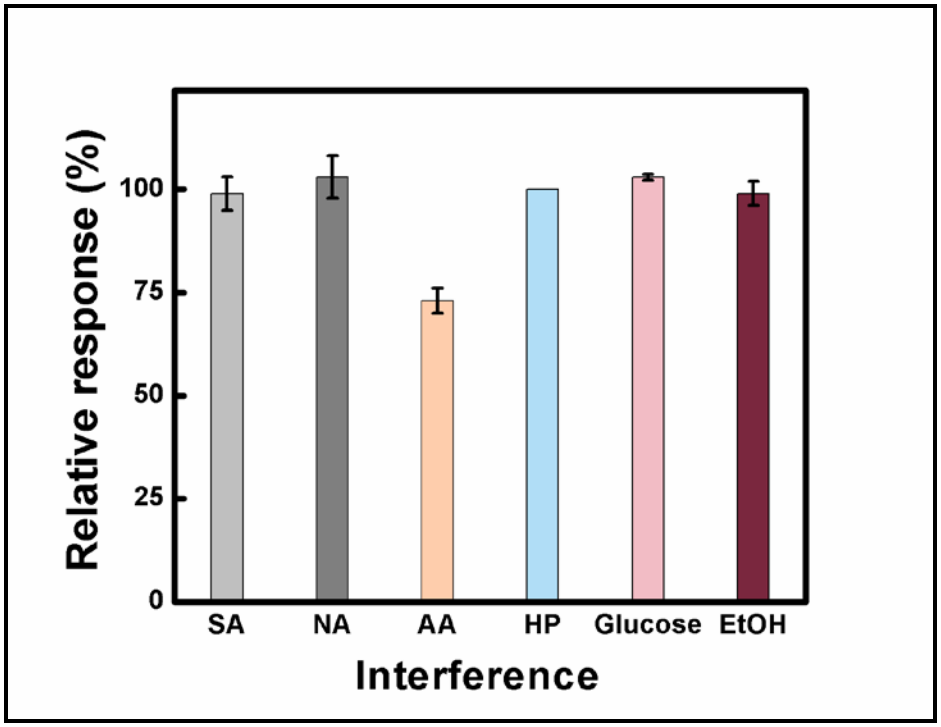

Figure 23. Relative response of PPy-CuNW/G electrode upon simultaneous addition of equivalent amount of H_2O_2 and different interference reagents (0.1 mM/0.1 mM). The electrode response for 0.1 mM H_2O_2 was taken as 100% and data points were average of three independent electrodes prepared at different time.

6.4. Open Circuit Potential (OCP) Measurement of the Polypyrrole Coated Copper Nanowire in Acidic Medium

Open circuit potential (V_{oc}) is one of the most widely accepted universal parameters to evaluate the anti-corrosion properties of certain materials. The higher the V_{oc} of a material, the harder the process to remove electrons from it, and its ability to resist corrosive oxidation would then defined to be stronger.[74] In order to evaluate the anti-corrosion properties of the as-

synthesized polypyrrole coated copper nanowire, a PPy-CuNW/G electrode was fabricated and subject to the electrochemical test under OCP condition.

6.4.1. Experimental Procedures for the OCP measurement

In a typical process, a PPy-CuNW/G electrode was fabricated according to the procedure mentioned in the context. Arbin instruments' BT 2000 testing system equipped with a conventional three electrode cell was used to perform the OCP test. A PPy-CuNW/G electrode was utilized as the working electrode while a platinum wire was used as the counter and Ag/AgCl as the reference. The experiment was conduct in 0.1 M HCl solution as the three electrode cell was meant to be immersed into the acidic solution. Open circuit condition was then applied to the electrode cell whereas no external current was passing through the cell and the voltage between the working and reference electrode was monitored continuously. The V_{oc} of the electrode was defined as the equilibrium potential corresponding to the steady-state plateau on the V_{oc} versus time plot. The control experiment, which the Cu particles synthesized in the same procedures as the polypyrrole coated wires but without the addition of pyrrole was utilized as the electrode material, was also performed, in order to evaluate the effect of polypyrrole coating on the V_{oc} of the copper wires underneath.

6.4.2. Results of the OCP measurement

The resulting V_{oc} versus time profile of the PPy-CuNW/G electrode and its control could be shown as Figure 24. However, it could be clearly observed from Figure 24 that the V_{oc} of PPy-CuNW/G electrode (0.10 V) has been enhanced substantially compared with the one of the Cu particles (-0.034 V), indicating the significant enhancement in anti-corrosion properties of the polypyrrole coated Cu nanowires compared to the uncoated Cu particles. This observation is

intriguing as it evidences the notable protecting effect of the polypyrrole coating layer for the Cu nanowires against the surrounding environment. Nonetheless, this intriguing enhancement of V_{oc} could be ascribed to the anti-corrosion protecting effect of the polypyrrole coating, possibly through the formation of a local electric field between the polypyrrole coating and the Cu wires, which restricts the electron movement within this field and increase the energy barrier for the corrosive cathodic reaction.[46] Therefore it could be inferred from the OCP test result that the polypyrrole coating could mean to protect the Cu nanowires underneath from the surrounding environment to a significant extent. In other words, the application and environmental stability of the Cu nanowires could be enhanced accordingly, which would be very important for the real-field practices of this Cu nanomaterial, as it is subject to be oxidized in air and well-known for the low stability.

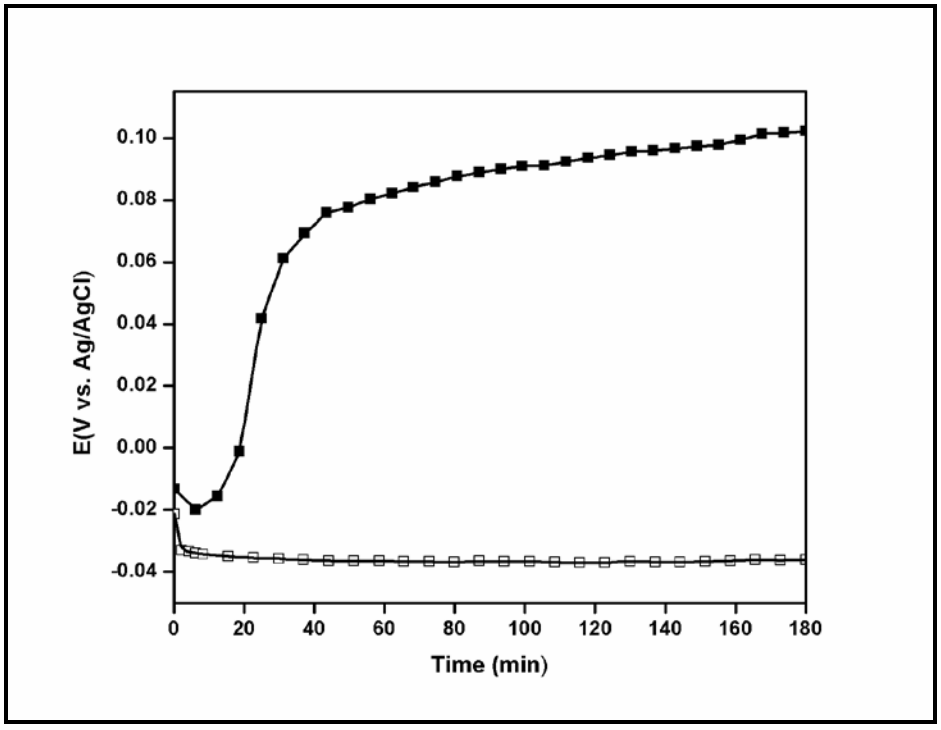

Figure 24. V_{oc} vs. time curves for PPy-CuNW (■) and Cu particles synthesized in the same condition without the addition of pyrrole (□) in 0.1 M HCl solution.

Chapter 7

Conclusions

In this thesis work, polypyrrole coated copper nanowires have been successfully synthesized using the solvothermal reduction process with hydrazine in a one-pot manner. The as-synthesized polypyrrole coated copper nanowires have possessed the average diameter of 350 nm and length around 10 μm. There exists a thin layer of polypyrrole coating on the surface of the Cu nanowires, the coating thickness is around 5-6 nm as measured using HRTEM. The as-synthesized copper naowires are single crystalline with a fringe space of 2.1 Å, and could be characterized as a piece of single crystal growing along the {110} direction with {111} facets exposed on the surface, as evidenced using SAED. The Cu nanowires possess typical X-ray diffraction pattern corresponding to the face-centered cubic (*fcc*) copper, with a calculated lattice constant of 3.614 Å, which is very close to that of pure copper (a=3.615 Å, JCPDS 4-836). However, a synergistic crystal growth and polymerization process is believed to induce the formation of the polypyrrole coating on copper nanowires. Polypyrrole should play both the reducing agent and structural directing agent role during the synthesis process, as it would coordinate with the cupric ions within the reaction solution and trigger the synergistic polymerization and crystal growth process through the ligand-to-metal charge transfer (LMCT) excitation. Eventually small copper particles capped with polypyrrole would form and they

would also serve as the seeds for the Cu nanowire growth through Oswald ripening process. As the crystal growth process is going on, the polymerization of pyrrole would not be stopped, and the as-formed polypyrrole would adsorb onto the surface of the growing wires through the coordination effect of its amine functional groups and the metallic surface, gradually forming the thin coating layer of polypyrrole. The electrochemical properties of the Cu nanowires exhibit subtle changes with the existence of the polypyrrole coating layer, as the cyclic voltammograms of the Cu wires are in good accord with the other copper based material, where typical redox peaks regarding the transitions of Cu^0/Cu(I), Cu(I)/Cu(II), Cu(II)/Cu(III) are displayed. On the other hand, the Cu wires exhibit notable catalytic properties for hydrogen reduction in PBS solution, as demonstrated by the corresponding cyclic voltammogram in PBS solution with the existence of H_2O_2. This phenomenon could be defined as the very base for the sensory ability of the Cu wires towards H_2O_2. The sensory properties of polypyrrole coated copper nanowire towards H_2O_2 have also been evaluated. A polypyrrole coated copper nanowire modified graphite electrode (PPy-CuNW/G) was fabricated and subjected to the potentiometric measurement in a conventional three electrode cell. The electrode shows sufficiently high sensitivity (180.65 mV/mM) towards each injection of H_2O_2 with relatively fast response time. It also exhibits excellent selectivity to various kinds of interfering agents such as sulfuric acid, nitric acid, glucose, and EtOH, as the electrode could retain at least 97% response to H_2O_2 in the presence of these agents. It has also been revealed that ascorbic acid would have a significant deteriorating effect for H_2O_2 detection, as a result of its anti-oxidant nature and possibly redox reaction with H_2O_2. Finally, the polypyrrole coated copper nanowires exhibit substantially enhanced V_{oc} in acidic medium compared to the uncoated samples, indicating the excellent protecting effect of the polypyrrole coating for the wires from the surrounding environment. This

finding could be very intriguing and significant for the field-applications of these copper nanomaterials in sensors, catalysts, or electronics, as they are well-known for poor environmental stability and to be readily oxidized in air.

References

(1) Shen, G.; Chen, P. C.; Ryu, K.; Zhou, C. Devices and Chemical Sensing Applications of Metal Oxide Nanowires. *J. Mater. Chem.* 2009, 19, 828-839.

(2) Chandra, M.; Xu, Q. Room Temperature Hydrogen Generation from Aqueous Ammonia-Borane Using Noble Metal Nano-Clusters as Highly Active Catalysts. *J. Power Sources* 2007, 168, 135-142.

(3) Varghese, O. K.; Grimes, C. A. Metal Oxide Nanoarchitectures for Environmental Sensing. *J. Nanosci. Nanotech.* 2003, 3, 277-293.

(4) Rao, C. N.; Kulkarni, G. U.; Govindaraj, A.; Satishkumar, B. C.; Thomas, P. J. Metal Nanoparticles, Nanowires, and Carbon Nanotubes**.** *Pure Appl. Chem.* 72, 21-33.

(5) Okumura, M.; Akita, T.; Haruta, M.; Wang, X.; Kajikawa, O.; Okada, O. Multi-Component Noble Metal Catalysts Prepared by Sequential Deposition Precipitation for Low Temperature Decomposition of Dioxin. *Appl. Catal. B: Environ.* 2003, 41, 43-52.

(6) Wiley, B.; Sun, Y.; Xia, Y. Synthesis of Silver Nanostructures with Controlled Shapes and Properties. *Acc. Chem. Res.* 2007, 40, 1067-1076.

(7) Astruc, D. *Nanoparticles and Catalysts.* 2008, WILEY-VCH.

(8) Farmer, J. A.; Campbell, C. T. Ceria Maintains Smaller Metal Catalyst Particles by Strong Metal-Support Bonding. *Science* 2010, 329, 933-936.

(9) Gao, T.; Meng, G.; Wang, Y.; Sun, S.; Zhang, L. Electrochemical Synthesis of Copper Nanowires. *J. Phys.: Condens. Mater* 2002, 14, 355-363.

(10) Ni, X.; Zhao, Q.; Zheng, H.; Li, B.; Song, J.; Zhang, D.; Zhang, X. A Novel Chemical Reduction Route towards the Synthesis of Crystalline Nickel Nanoflowers from a Mixed Source. *Eur. J. Inorg. Chem.* 2005, 4788-4793.

(11) Puntes, V. F.; Krishnan, K. M.; Alivisatos, A. P. Colloidal Nanocrystal Shape and Size Control: The Case of Cobalt. *Science* 2001, 291, 2115-2117.

(12) Zach, M. P.; Ng, K. H.; Penner, R. M. Molybdenum Nanowires by Electrodeposition. *Science* 2000, 290, 2120-2123.

(13) Chang, Y.; Lye, M. L.; Zeng, H. C. Large-Scale Synthesis of High-Quality Ultralong Copper Nanowires. *Langmuir* 2005, 21, 3746-3748.

(14) Yazyev, O. V.; Louie, S. G. Electronic Transport in Polycrystalline Graphene. *Nature Materials* 2010, 9, 806-809.

(15) Tao, A. R.; Habas, S.; Yang, P. Shape Control of Colloidal Metal Nanocrystals. *Small* 2008, 4, 310-325.

(16) Bandyopadhyay, S. K.; Pal, A. K. The Effect of Grain Boundary Scattering on the Electron Transport of Aluminium Films. *J. Phys. D: Appl. Phys.* 1979, 12, 953-959.

(17) Schrinner, M.; Ballauff, M.; Talmon, Y.; Kauffmann, Y.; Thun, J.; Moller, M.; Breu, J. Single Nanocrystals of Platinum Prepared by Partial Dissolution of Au-Pt Nanoalloys. *Science* 2009, 323, 617-620.

(18) Lee, Y.; Choi, J.; Lee, K. J.; Stott, N. E.; Kim, D. Large-Scale Synthesis of Copper Nanoparticles by Chemically Controlled Reduction for Applications of Inkjet-Printed Electronics. *Nanotechnology* 2008, 19, 415604.

(19) Mohl, M.; Pusztai, P.; Kukovecz, A.; Konya, Z. Low-Temperature Large-Scale Synthesis and Electrical Testing of Ultralong Copper Nanowires. *Langmuir* 2010, 26, 16496-16502.

(20) Liu, Z.; Bando, Y. A Novel Method for Preparing Copper Nanorods and Nanowires. *Adv. Mater*. 2003, 15, 303-305.

(21) Wang, Y.; Chen, P.; Liu, M. Synthesis of Well-Defined Copper Nanocubes by a One-Pot Solution Process. *Nanotechnology* 2006, 17, 6000-6006.

(22) Jain, P. K.; Huang, X.; El-Sayed, I. H. Review of Some Interesting Surface Plasmon Resonance-Enhanced Properties of Noble Metal Nanoparticles and Their Applications to Biosystems. *Plasmonics* 2007, 2, 107-118.

(23) Star, A.; Joshi, V.; Skarupo, S.; Thomas, D.; Gabriel, J. C. Gas Sensor Array Based on Metal-Decorated Carbon Nanotubes. *J. Phys. Chem. B* 2006, 110, 21014-21020.

(24) Lim, J. K.; Joo, S. W. Gold Nanoparticle-Based pH Sensor in Highly Alkaline Region at pH > 11: Surface-Enhanced Raman Scattering Study. *Appl. Spectrosc.* 2006, 60, 847-852.

(25) Alivisatos, P. The Use of Nanocrystals in Biological Detection. *Nat. Biotechnol.* 2004, 22, 47-52

(26) Melosh, N. A.; Boukai, A.; Diana, F.; Gerardot, B.; Badolato, A.; Petroff, P. M.; Heath, J. R. Ultrahigh-Density Nanowire Lattices and Circuits. *Science* 2003, 300, 112-115.

(27) Wang, S.; Wang, X.; Jiang, S. Controllable Self-Assembly of Pd Nanowire Networks as Highly Active Electrocatalysts for Direct Formic Acid Fuel Cells. *Nanotechnology* 2008, 19, 455602.

(28) Christopher, P.; Linic, S. Engineering Selectivity in Heterogeneous Catalysis: Ag Nanowires as Selective Ethylene Epoxidation Catalysts. *J. Am. Chem. Soc.* 2008, 130, 11264-11265.

(29) Liu, Z.; Yang, Y.; Liang, J.; Hu, Z.; Li, S.; Peng, S.; Qian, Y. Synthesis of Copper Nanowires via a Complex-Surfactant-Assisted Hydrothermal Reduction Process. *J. Phys. Chem. B* 2003, 107, 12658-12661.

(30) Enculescu, I.; Toimil-Molares, M. E.; Zet, C.; Drub, M.; Westerberg, L.; Neumann, R.; Spohr, R. Current Perpendicular to Plane Single-Nanowire GMR Sensor. *Appl. Phys. A* 2007, 86, 43-48.

(31) Kevin, M.; Ong, W. L.; Lee, G. H.; Ho, G. W. Formation of Hybrid Structures: Copper Oxide Nanocrystals Templated on Ultralong Copper Nanowires for Open Network Sensing at Room Temperature. *Nanotechnology* 2011, 22, 235701.

(32) Pei, L.; Wang, J.; Yang, L.; Dong, Y.; Wang, S.; Fan, C.; Hu, J.; Zhang, Q. Preparation of Copper Germanate Nanowires with Good Electrochemical Sensing Properties. *Cryst. Res. Technol.* 2011, 46, 103-112.

(33) Li, C.; He, H.; Bogozi, A.; Bunch, J. S.; Tao, N. Molecular Detection Based on Conductance Quantization of Nanowires. *J. Appl. Phys. Lett.* 2000, 76, 1333-1335.

(34) Ateh, D. D.; Navsaria, H. A.; Vadgama, P. Polypyrrole-Based Conducting Polymers and Interactions with Biological Tissues. *J. R. Soc. Interface* 2006, 3, 741-752.

(35) Li, C.; Bai, H.; Shi, G. Conducting Polymer Nanomaterials: Electrosynthesis and Applications. *Chem. Soc. Rev.* 2009, 38, 2397-2409.

(36) Gorman, C. B.; Biebuyck, H. A.; Whitesides, G. M. Fabrication of Patterned, Electrically Conducting Polypyrrole Using a Self-Assembled Monolayer: A Route to All-Organic Circuits. *Chem. Mater.* 1995, 7, 526-529.

(37) Gangopadhyay, R.; De, A. Conducting Polymer Nanocomposites: A Brief Overview. *Chem. Mater.* 2000, 12, 608-622.

(38) Kanatzidis, M. G.; Tonge, L. M.; Marks, T. J. In Situ Intercalative Polymerization of Pyrrole in FeOCl: A New Class of Layered, Conducting Polymer-Inorganic Hybrid Materials. *J. Am. Chem. Soc.* 1987, 109, 3797-3799.

(39) Bredas, J. L.; Street, G. B. Polarons, Bipolarons, and Solitons in Conducting Polymers. *Acc. Chem. Res.* 1985, 18, 309-315.

(40) Macdiarmid, A. G. Synthetic Metals: A Novel Role for Organic Polymers. *Angew. Chem. Int. Ed.* 2001, 40, 2581-2590.

(41) Sadki, S.; Schottland, P.; Brodie, N.; Sabouraud, G. The Mechanisms of Pyrrole Electropolymerization. *Chem. Soc. Rev.* 2000, 29, 283-293.

(42) Liu, X.; Ly, J.; Han, S.; Zhang, D.; Requicha, A.; Thompson, M. E.; Zhou, C. Synthesis and Electronic Properties of Individual Single-Walled Carbon Nanotube/Polypyrrole Composite Nanocables. *Adv. Mater.* 2005, 17, 2727-2732.

(43) Lascelles, S. F.; Armes, S. P. Synthesis and Characterization of Micrometre-Sized, Polypyrrole-Coated Polystyrene Latexes. *J. Mater. Chem.* 1997, 7, 1339-1347.

(44) Chen, G. Z.; Shaffer, M. S.; Coleby, D.; Dixon, G.; Zhou, W.; Fray, D. J.; Windle, A. H. Carbon Nanotube and Polypyrrole Composites: Coating and Doping. *Adv. Mater.* 2000, 12, 522-526.

(45) Riaz, U.; Ashraf, S. M.; Ahmad, S. High Performance Corrosion Protective DGEBA/Polypyrrole Composite Coatings. *Prog. Org. Coat.* 2007, 59, 138-245.

(46) Truong, V. T.; Lai, P. K.; Moore, B. T.; Muscat, R. F.; Russo, M. S. Corrosion Protection of Magnesium by Electroactive Polypyrrolerpaint Coatings. *Synth. Met.* 2000, 110, 7-15.

(47) Sasso, C.; Zeno, E.; Petit-Conil, M.; Chaussy, D.; Belgacem, M. N.; Tapin-Lingua, S.; Beneventi, D. Highly Conducting Polypyrrole/Cellulose Nanocomposite Films with Enhanced Mechanical Properties. *Macromol. Mater. Eng*. 2010, 295, 934-941.

(48) Tansley, T. L; Maddison, D. S. Conductivity Degradation in Oxygen-Aged Polypyrrole. *J. Appl. Phys*. 1991, 69, 7711-7713.

(49) Tian, B.; Zerbi, G. Lattice Dynamics and Vibrational Spectra of Polypyrrole. *J. Chem. Phys.* 1990, 92, 3886-3891.

(50) Kostic, R.; Rakovic, D.; Stepanyan, S. A.; Davidova, I. E.; Gribov, L. A. Vibrational Spectroscopy of Polypyrrole, Theoretical Study. *J. Chem. Phys.* 1995, 102, 3104-3109.

(51) Huang, C. L.; Matijeric, E. J. Coating of Uniform Inorganic Particles with Polymers. *J. Mater. Res.* 1995, 10, 1327-1336.

(52) Biondi, M. A.; Guobadia, A. I. Infrared Absorption of Aluminum, Copper, Lead, and Nickel at 4.2°K. *Phys. Rev.* 1968, 166, 667-673.

(53) Lisiecki, I.; Pileni, M. P. Copper Metallic Particles Synthesized "in Situ" in Reverse Micelles: Influence of Various Parameters on the Size of the Particles. *J. Phys. Chem.* 1995, 99, 5077-5082.

(54) Xia, Y.; Macdiarmid, A. G. Camphorsulfonic Acid Fully Doped Polyaniline Emeraldine Salt: In situ Observation of Electronic and Conformational Changes Induced by Organic Vapors by an Ultraviolet/Visible/Near-Infrared Spectroscopic Method. *Macromolecules* 1994, 27, 7212-7214.

(55) Minami, T.; Nishiyabu, R.; Iyoda, M.; Kubo, Y. Shape-Controllable Gold Nanocrystallization Using an Amphiphilic Polythiophene. *Chem. Commun.* 2010, 46, 8603-8605.

(56) Sigel, H.; Martin, R. B. Coordinating Properties of the Amide Bond: Stability and Structure of Metal Ion Complexes of Peptides and Related Ligands. *Chem. Rev.* 1982, 82, 385-426.

(57) Fawcett, T. G.; Bernarducci, E. E.; Krogh-Jespersen, K.; Schugar, H. J. Charge-Transfer Absorptions of Copper(II)-Imidazole and Copper(II)-Imidazolate Chromophores. *J. Am. Chem. Soc.* 1980, 102, 2598-2604.

(58) Miskowski, V. M.; Thich, J. A.; Solomon, R.; Schugar, H. J. Electronic Spectra of Substituted Copper(II) Thioether Complexes. *J. Am. Chem. Soc.* 1976, 98, 8344-8350.

(59) Schoonover, J. R.; Strouse, G. F. Time-Resolved Vibrational Spectroscopy of Electronically Excited Inorganic Complexes in Solution. *Chem. Rev.* 1998, 98, 1335-1355.

(60) Wu, S.; Meng, S. Preparation of Micron Size Copper Powder with Chemical Reduction Method. *Materials Letters* 2006, 60, 2438-2442.

(61) Mullen, P. A.; Orloff, M. K. Ultraviolet Absorption Spectrum of Pyrrole Vapor Including the Observation of Low-Energy Transitions in the Far Ultraviolet. *J. Chem. Phys* 1969, 51, 2276-2278.

(62) Manohar, S. K.; Macdiarmid, A. G.; Epstein, A. J. Polyaniline: Pernigraniline, An Isolable Intermediate in Conventional Chemical Synthesis of Emeraldine. *Synthe. Met.* 1991, 41, 711-714.

(63) Myers, R. E. Chemical Oxidative Polymerization as a Synthetic Route to Electrically Conducting Polymer. *J. Electron. Mater.* 1986, 15, 61-69.

(64) Huang, C. H.; Stone, A. T. Transformation of the Plant Growth Regulator Daminozide (Alar) and Structurally Related Compounds with Cu(II) Ions: Oxidation versus Hydrolysis. *Environ. Sci. Technol.* 2003, 37, 1829-1837.

(65) Creighton, H. J. M. The Action of Solutions of Alkali Hydroxides on Copper Oxide and on Copper, and the Existence of Salts of Cupric Acid. *J. Am. Chem. Soc.* 1923, 45, 1237-1243.

(66) Roosen, A. R. Carter, W. C. Simulations of Microstructural Evolution: Anisotropic Growth and Coarsening. *Physica A* 1998, 261, 232-247.

(67) Inoue, M. B.; Nebesny, K. W.; Fernando, Q. Complexation of Electroconducting Polypyrrole with Copper. *Synthe. Met.* 1990,38, 205-212.

(68) Bakker, E. Electrochemical Sensors. *Anal. Chem*. 2004, 76, 3285-3298.

(69) Bakker, E.; Pretsch, E. Potentiometric Sensors for Trace-Level Analysis. *Trends Analyt Chem.* 2005, 24, 199-207.

(70) Smyth, M. R. *Analytical Voltammetry*. Elsevier, 1992.

(71) Kuwana, T.; Marioli, J. M. Electrochemical Characterization of Carbohydrate Oxidation at Copper Electrodes. *Electrochimica Acta* 1992, 37, 1187-1197.

(72) Grujicic, D.; Pesic, B. Electrodeposition of Copper: the Nucleation Mechanisms. *Electrochimica Acta* 2002, 47, 2901-2912.

(73) Lowry, J. P.; O'Neill, R. D. Homogeneous Mechanism of Ascorbic Acid Interference in Hydrogen Peroxide Detection at Enzyme-Modified Electrodes. *Anal. Chem.* 1992, 64, 456-459.

(74) Mirmohseni, A.; Oladegaragoze, A. Anti-Corrosive Properties of Polyaniline Coating on Iron. *Synthe. Met.* 2000, 114, 105-108.